Energy Conversion and Management 273 (2022) 116426

Contents lists available at ScienceDirect

Energy Conversion and Management

journal homepage: www.elsevier.com/locate/enconman

Operational optimisation of an air-source heat pump system with thermal energy storage for domestic applications

Andreas V. Olympios [a], Paul Sapin [a], James Freeman [b], Christopher Olkis [b], Christos N. Markides [a,*]

[a] Clean Energy Processes (CEP) Laboratory and Centre for Process Systems Engineering (CPSE), Department of Chemical Engineering, Imperial College London, London SW7 2AZ, UK

[b] Mitsubishi Electric R&D Centre Europe B.V., 17 Firth Road, Houston Industrial Estate, Livingston EH54 5DJ, UK

ARTICLE INFO

Keywords:
Domestic heating
Genetic algorithm
Heat pump
Optimisation
Phase-change material
Thermal energy storage

ABSTRACT

Electricity-driven air-source heat pumps are a promising element of the transition to lower-carbon energy systems. In this work, operational optimisation is performed of an air-source heat pump system aimed at providing space heating and domestic hot water to a single-family dwelling. The novelty of this work lies in the development of comprehensive thermal network models of two different system configurations: (i) a standard configuration of a heat pump system coupled to a hot-water cylinder; and (ii) an advanced configuration of a heat pump system coupled to two phase-change material thermal stores. Three different objective functions (operational cost, coefficient of performance, and self-sufficiency from a locally installed solar-PV system) are investigated and the proposed mixed-integer, non-linear optimisation problems are solved by employing a genetic algorithm. Simulations are conducted at two carefully selected European locations with different climate characteristics (Oban in Scotland, UK, and Munich in Southern Germany) over four seasons represented by typical weather weeks. Comparison of key results against a conventional operating strategy reveals that the use of smart operational strategies for the operation of the heat pump and thermal stores can lead to considerable economic savings for consumers and significant performance improvements over the system lifetime. Optimising the operation of the standard configuration leads to average annual cost savings of up to 22% and 20% at the UK and German locations, respectively. The optimisation of the advanced configuration with the two PCM stores shows even higher potential for economic savings – up to 39% and 29% per year at the respective locations – as this configuration allows for greater operational flexibility, and high-electricity-price periods can be almost completely avoided. Depending on the objective function, configuration and location, the system seasonal coefficient of performance varies between 2.4 and 2.8. Lastly, a significant (up to four-times) increase in the fraction of heat pump energy demand covered by an appropriately-sized rooftop PV system is demonstrated, increasing from 8% to 34% at the UK location and from 6% to 24% at the German location. The analysis highlights trade-offs between the objective functions, while the time-resolved results can be used to guide the future development of smart controllers for these applications.

1. Introduction

Heating is one of the largest causes of energy consumption in our societies. In Europe, heating and cooling account for 50 % of total energy consumption [1], while in the UK, more than 40 % of the energy consumption is attributed to space heating and hot water provision for buildings [2]. Although emissions of greenhouse gases have been 20 % lower than in 1990, drastic action is required to reach net-zero carbon emissions by 2050. Many countries have enacted the net-zero target by law [3,4] to meet the Paris Agreement's objectives [5]. In the Heat and Buildings Strategy published by the UK government in late 2021, it is stated that the installation of gas boilers should be phased out from 2035 [6].

1.1. Heat pumps and demand-side response

The "Heat Roadmap Europe" (HRE) [7] predicts that the CO_2

* Corresponding author.
E-mail address: c.markides@imperial.ac.uk (C.N. Markides).

https://doi.org/10.1016/j.enconman.2022.116426
Received 8 August 2022; Received in revised form 21 October 2022; Accepted 27 October 2022
Available online 10 November 2022

Nomenclature

Acronyms

ASHP	air-source heat pump
COP	coefficient of performance
DHW	domestic hot water
DSR	demand-side response
EU	European Union
MINLP	mixed-integer non-linear problem
PCM	phase-change material
PV	photovoltaic
SH	space heating
TES	thermal energy storage

Greek symbols

α	binary (on/off)
γ	temperature coefficient (1/K)
ε	heat exchanger effectiveness (-)
η	efficiency (-)
λ	thermal conductivity (W/m/K)
ρ	density (kg/m^3)

Symbols

A	area (m^2)
C	thermal capacitance (J/K)
c_p	specific heat capacity (J/kg/K)
G	thermal conductance (W/K)
H	height (m)
I	irradiance (W/m^2)
L	specific latent heat (J/kg)
m	mass (kg)
$\dot{m}$	mass flow rate (kg/s)
n	number (-)
Obj	objective function (-)
P	price (£/kWh)
$\dot{Q}$	heat flow (W)
R	radius (m)
T	temperature (K)
t	time (s)
$\dot{W}$	power (W)

Subscripts

amb	ambient temperature
c	cylinder
cold	cold side of the cylinder
cost	operational cost
d	demand
EH	electric heater
elec	electricity
em	heat emitters
env	building envelope
ext	external environment
gt	global tilt
hot	hot side of the cylinder
HP	heat pump
ig	internal gains (e.g., appliances)
imp	imported electricity
in	inlet/input
int	building internal space
inv	inverter
loss	thermal loss to surroundings
mains	cold mains water
max	maximum
min	minimum
nom	nominal
out	outlet/output
pan	panel
p	pipe in primary loop
PL	primary loop
s	solar gain
sg	solar gains
SL	secondary loop
suff	self-sufficiency
sys	heat pump & electric heater system
w	water
vent	ventilation

emissions produced in Europe's heating and cooling sector can be reduced by more than 85 % by 2050 compared to 1990 using only known technologies. As stated in the roadmap, electricity-driven heat pumps will be key to facilitate the switch from traditional oil and gas boilers and thus enable the efficient use of resources. Therefore, they constitute one of the main pathways to decarbonise the domestic heating sector [8].

Electricity-driven heat pumps do not produce greenhouse gases at point-of-use in the household. In addition, heat pumps are formally classified as renewable energy devices. If a significant part of electricity required can be produced using renewable energy sources, heat pump technology can be established as a low-carbon heating solution, even from a system perspective. The carbon intensity of electricity grids, which refers to the amount of CO_2 released to the atmosphere per unit of electricity produced, has been rapidly decreasing in recent years. In the European Union (EU), for example, the carbon intensity experienced an average decrease of more than 20 % in the last 10 years [9], while it has reduced by more than 50 % in the UK [10].

Heat pumps utilise mechanical work to transfer heat from a cold to a hot region, extracting heat from the environment [11], which can be used in domestic applications to provide both domestic hot water (DHW) and space heating (SH). This mature technology has experienced significant market growth in recent years (more than 10 % per year since 2014) [12]. However, the heat pump market share is still low at about 14.9 million units in the EU and 0.25 million units in the UK [12]. The main reasons for this include: (i) large capital costs (which can vary between 300 £/kW$_{th}$ and 650 £/kW$_{th}$ depending on the size and specifications [13]); (ii) lack of consumer awareness on the reliability and comfort that these systems can provide; and (iii) lack of information regarding the degree to which operational savings can be achieved.

The fundamental issues associated with the intermittency of renewable generation indicate that demand-side response (DSR) will have a vital role to play in near-future electricity systems [14,15]. Through price-based programs, end-users with flexible loads can respond to grid requirements, shifting some of the electricity that they import from high-demand to low-demand periods, supporting the smooth transition of the current system to a more adaptable grid and encouraging the uptake of more renewable generation technologies [16]. At the same time, end-users can benefit from reduced operational costs using smart meters and variable-price electricity tariffs [17,18].

When coupled with thermal energy storage (TES) in distributed energy systems, heat pumps can be operated flexibly, potentially showing great value in providing DSR [19,20]. Heat pumps can be switched on during low-electricity-price periods to charge the TES device, which can be discharged later to meet up demand when electricity prices are higher. TES devices act as a buffer between demand and supply, so that

importing electricity during high-electricity-price periods can be avoided.

TES devices can be classified into sensible-heat, latent-heat, or thermochemical storage systems [21], with sensible-heat storage using hot water being the most common in the case of DHW and SH applications in buildings. Thermochemical TES technologies promise the highest energy densities, but are also at the earliest development stages amongst these options. On the other hand, latent-heat TES systems based on phase-change materials (PCMs) have gained commercial interest and various products are now available on the market [22–24]. PCM-based thermal stores exhibit higher energy densities than hot-water cylinders, and can store and recover heat in a small temperature band [25].

1.2. Operation optimisation of domestic heat pump with thermal storage for cost minimisation

Several studies investigated heat pump load-shifting using thermal storage. Renaldi et al. [26] predicted that, despite the price of gas being significantly lower than that of electricity, optimising the operation of an air-source heat pump (ASHP) in a typical house in Greater London based on variable electricity tariffs allows for a 6-% reduction in operational costs compared to using a gas boiler. The authors showed that, in conjunction with the Renewable Heating Incentive provided by the UK government, heat pumps can be a competitive option. By considering hourly time steps and simulating a whole year, the optimal volume of the hot-water cylinder was found to vary between 210 L and 300 L depending on the type of electricity tariff. Arteconi et al. [27] used a detached house in Northern Ireland as a case study, demonstrating that time-of-use electricity tariffs play a major part in convincing end-users to switch off their ASHP during peak-demand-periods (16:00–19:00). In addition, the use of radiators as heat emitters would require a 500-L thermal-storage volume (based on a stratified hot-water cylinder) to guarantee that the heat pump is switched off during those times and that SH is always provided. Furthermore, Fischer et al. [28] compared different control strategies for a PV-assisted ASHP using a multi-family (12-person) house in Potsdam, Germany, as a case study. Using a thermal storage volume of 3000 L, the use of model predictive control was shown to reduce operational costs by more than 10 % when compared to simple rule-based control strategies.

In the work of Le et al. [29], the authors focused on a cascade ASHP system and chose Northern Ireland as the case study as well, presenting high operational cost savings compared to oil boilers (16–34 %). The work was based on a TES device made of a hot-water cylinder of volume varying between 600 L and 1100 L and concluded that the best times to charge the storage are at 03:00 in the morning (due to low electricity prices) and 14:00 in the afternoon (due to high ambient temperature).

Phase-change materials (PCM) are promoted in literature as a method to provide heat pump flexibility at domestic scale. In the work of Cabrol and Rowley [30], the operation of an ASHP was optimised to show that, using an underfloor-heating system with a concrete floor slab containing PCM, cost savings can reach up to 50 % compared to the use of a gas boiler for different UK locations. Furthermore, in the work of Kelly et al. [31], the results show that a 1000-L hot-water cylinder or a 500-L PCM thermal store are necessary to switch the heat pump operation to off-peak periods in order to meet DHW and SH demand.

In summary, most studies conclude that a relatively large thermal storage device is required in order to obtain meaningful economic savings by operation time-shifting (500-L cylinder in Ref. [27], 600–1100 L cylinder in Ref. [29], 1000-L cylinder or 500-L PCM thermal store in Ref. [31]). It is also important to consider that DHW demand often experiences substantial fluctuations with time, which means that capturing the instantaneous peaks requires a high temporal resolution [32], otherwise the storage volume required to meet all demand at all times may be underestimated (e.g., 210–300 L cylinder in Ref. [26] using hourly resolution). The Hot Water Association in the UK states that a typical four-person household often uses around 200 L of hot water per day [33], and manufacturers often suggest that cylinders should allow ~ 50 L of water per person per day [34]. Installing much larger cylinders (e.g., 500–1000 L), which is suggested in many of the above studies, is only an interesting option for large households with no space limitations. An assessment of the degree to which smart operation strategies can lead to economic savings even when using storage volumes applicable to small- or medium-sized dwellings has not been performed yet.

1.3. Other operation objectives

1.3.1. Heat pump performance

Smart control strategies can be used not only to minimise operational costs, but also to operate heat pump systems whenever the environmental conditions are favourable, improving the overall performance and minimising the total electricity consumption. The performance of heat pumps largely depends on operating conditions (weather, demand typology, etc.) and is rated using the coefficient of performance (COP), defined as the ratio of the heat output to the electricity input.

The COP can be improved by time-shifting operation to minimise the temperature difference between the heat-source fluid (ambient air in the case of ASHPs) and heat-sink fluid (heated water) [35]. For example, the TES device can be charged whenever the ambient temperature is relatively high (which corresponds to a high heat pump performance), and the system can be turned off during cold periods, increasing the overall COP over the daily or annual period. In the work of Nouri et al. [36], different configurations of a ground-source heat pump assisted by a solar thermal collector are compared based on the annual COP, demonstrating that CO_2 emissions can be reduced by more than 50 % compared to conventional gas-driven heating systems. Various tools have been developed to optimally design heat pumps and/or predict their seasonal energy performance [37,38]. However, less effort has been devoted to identifying smart control strategies for energy performance maximisation.

1.3.2. PV self-sufficiency

If electricity is produced locally from a renewable-electricity source, heat pumps can be also operated to maximise self-sufficiency, which is defined as the proportion of electricity locally used that is not imported from the wider-area grid. Increasing the self-sufficiency of buildings is one of the targets set by many EU countries [39] and is an important topic in energy-community and microgrid applications [40]. A solar-house prototype was developed in Madrid, Spain, to be an energy self-sufficient house based on passive design strategies [41], and self-sufficiency in the case of heating is achieved through the use of two hot-water cylinders (one for the solar collectors and one for the heat pump). Furthermore, in the work of Huang et al. [42], a system of PV collectors, heat pumps, thermal storage and electric vehicles for a group of residential buildings is analysed. Various techno-economic performance indicators are compared, showing that aggregating the demand of buildings leads to smoother demand profiles than those of individual homes, allowing for a greater portion of the generated PV power to be locally used.

In the work of Iwafune et al. [43], the authors reported that self-consumption, the proportion of electricity produced from a PV system of an average household in Japan that is internally used, can be increased by more than 10 % when optimising the heat pump operation. Similarly, in the work of Fischer [28], this proportion was shown to increase by more than 5 % using model predictive control. The objective function in the above studies was the operational cost.

Langer et al. [44] compared the effectiveness of self-consumption and self-sufficiency as alternative objective functions to operation cost for the optimal operation of a PV-assisted ASHP in a four-person house in Germany. The results showed that using self-consumption as the objective function leads to a significant reduction of 9 % in cost savings compared to using operational cost. On the other hand, the use of self-sufficiency as the objective function only marginally reduces cost

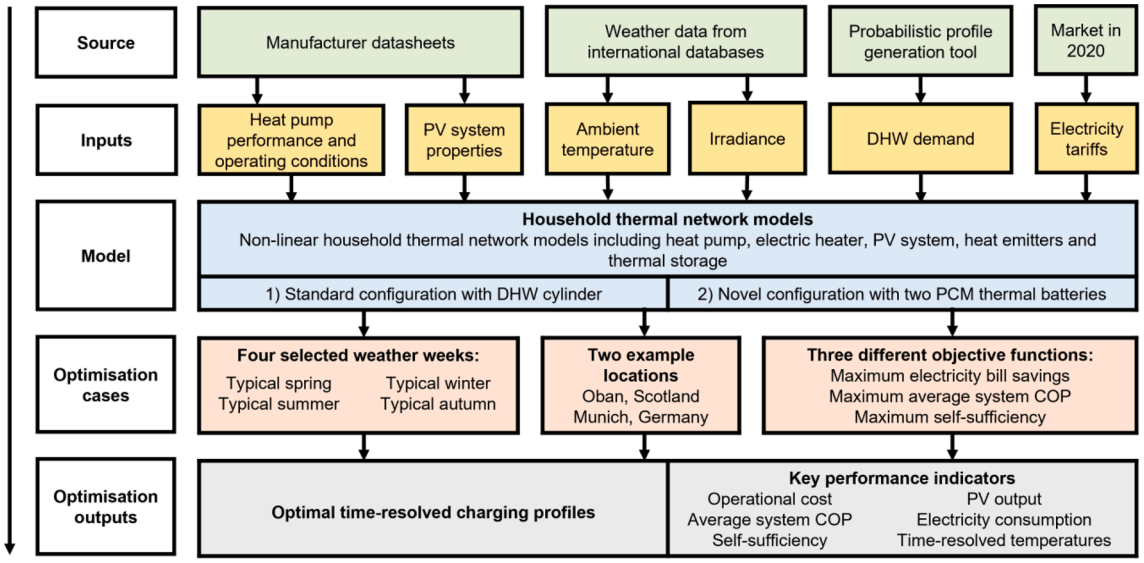

Fig. 1. General structure of the developed framework. Two different heat-pump system configurations are investigated for four selected weather weeks, two different locations and three different objective functions.

savings (2 %) compared to using operational cost and leads to decreased solution times for the optimisation problem. In the near future, many new built-homes will be likely equipped with solar-assisted heat pumps [45–47], and, in conjunction with energy bill savings and technology performance, self-sufficiency is an objective that merits further investigation.

1.4. Contributions

While significant work has been done in the areas of domestic heating and heat pump operation optimisation, there remain some gaps in the literature. In detail, there is a need to assess the potential to reduce consumer costs and improve efficiency in domestic heating applications through the use of: (i) smart operation strategies in small- or medium-sized dwellings which do not have the option of very large storage volumes; (ii) PCMs as an alternative TES method to sensible-heat storage; and (iii) objective functions other than operational cost (heat pump performance, PV self-sufficiency).

In this work we assess the potential for optimising the charging schedule of a domestic ASHP system with a TES device for three different objectives:

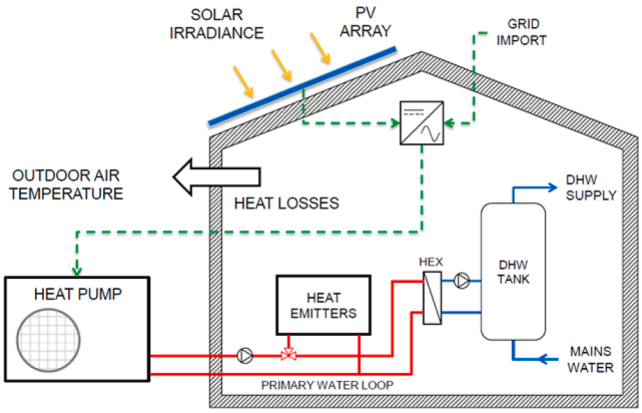

Fig. 2. Standard configuration of a heat pump system coupled with heat emitters for the provision of SH and a hot-water cylinder for the provision of DHW. A solar-PV system is installed to produce electricity locally.

(i) maximisation of energy bill savings based on a domestic time-of-use electricity price tariff;
(ii) maximisation of the heat pump system COP based on the daily swing in outdoor temperatures; and
(iii) maximisation of self-sufficiency from a locally installed solar-PV system.

The first novelty of this work lies in the development of comprehensive thermal network models for a typical house for two different system configurations: (i) a standard configuration of a domestic ASHP system coupled to a hot-water cylinder; and (ii) an advanced configuration based on PCM thermal storage. The developed optimisation problems are constrained mixed-integer non-linear programs (MINLP) and are solved using a genetic algorithm.

In this work, thermal storage volumes typical of heat pump products for small- or medium-sized dwellings (200 L) are assumed for the two configurations, aiming to demonstrate whether economic savings can be achieved even in the presence of significant space limitations. The results of the operational optimisation are compared to a baseline case which is based on a standard configuration of a domestic ASHP system coupled to a hot-water cylinder, aiming to identify the potential savings that can be obtained using a smart operation strategy compared to a typical "reactive" approach based on thermostatic control.

Another contribution of this work is that all scenarios are conducted for two different, carefully selected, locations: Oban in Scotland, UK, a location which experiences low solar irradiance and mild temperatures, and Munich in Southern Germany, which is a sunny location with large diurnal and seasonal temperature variations. Applicable energy price tariffs are also considered for the two countries, so as to assess the improvement potential in both locations (with specific energy prices and climates) for the different objective functions considered in this work.

The problem definition, the thermal network models and the model inputs and assumptions are presented in Section 2. The analysis and comparison of the different optimisation cases is presented in Section 3. This includes an assessment of the potential improvements in energy bill savings, system COP and self-sufficiency, as well as insights into the strategic charging and discharging scheduling options. Section 4 provides concluding remarks.

2. Methods

The general structure of the framework developed in this paper is

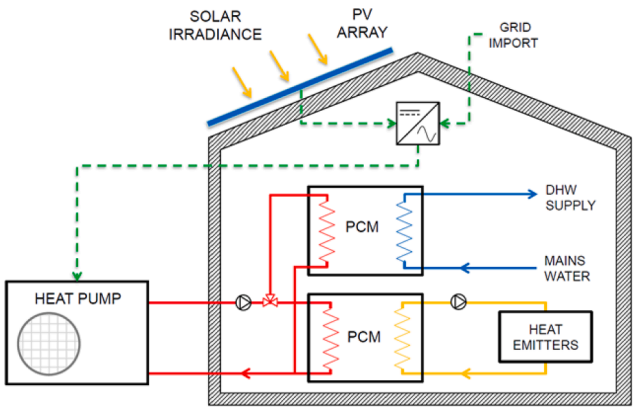

Fig. 3. Advanced configuration of a heat pump system coupled with two separate PCM thermal stores: one for the provision of SH and one for the provision of DHW. A solar-PV system is installed to produce electricity locally.

presented in Fig. 1. Technical information from manufacturer datasheets is used to develop simple performance models of the PV and heat pump systems and weather data is collected for the locations under investigation (Oban, UK, and Munich, Southern Germany). A probabilistic DHW demand profile is generated and electricity tariffs for the two countries based on the market situation in Europe in 2020 are used. Using the developed thermal network models, the charging-schedule profiles and key performance indicators are determined for the two configurations (one based on a standard heat-pump system coupled to a hot-water cylinder and one based on an advanced system with PCM storage) for four selected typical weather weeks and three objective functions. In this section, the configurations, thermal networks and model inputs are presented.

2.1. Heat-pump system configurations

The first system configuration, shown in Fig. 2, involves the following main components: an ASHP, an array of heat emitters, a hot-water cylinder and a solar-PV system. This represents one of the most common configurations currently found on the heat pump market [48,49], with a 3-way, 2-position valve allowing the ASHP to switch between providing SH via the heat emitters (radiators) or charging the hot-water cylinder via a heat exchanger located in the indoor unit of the heat pump system. Hot water is drawn from the top of the cylinder whenever there is DHW demand, and cold mains water simultaneously enters from the bottom. The house experiences heat losses to the outside environment.

The electricity produced by the solar-PV system is used to drive the heat pump, while additional (excess) electricity required is imported from the grid. It is assumed in this work that end-users cannot benefit from selling electricity to the grid. In reality, grid operators can reward users economically for their exports of PV-produced electricity to the grid. However, the reward for exporting electricity in the UK and Europe has been varied and highly volatile, and since such schemes change every few years and the uncertainty related to their future development is high, it was decided not to consider this possibility in this work. Therefore, the cost savings reported here are conservative: if end-users are eligible for monetary incentives for exporting electricity, the potential for cost savings associated from smart operation of the heat pump system can be higher than reported.

The ASHP system includes a backup electric heater, also commonly referred to as a booster heater, to provide supplementary heating of the heat-transfer fluid when required. The heater is available in most domestic heating systems [48,50] and is a necessary component when ambient temperatures drop outside the operating conditions achievable by the heat pump.

The second system configuration, shown in Fig. 3, includes a heat pump, two separate PCM thermal stores, an array of heat emitters and a solar-PV system. The main differences to the first configuration are that the hot-water cylinder has been replaced by a PCM thermal store and the ASHP does not provide SH directly, as a second PCM thermal store acts as a buffer between heat supplied by the ASHP and SH demand. The solar-PV system is operated in the same way and an electric booster heater is again included for supplementary heating.

2.2. Thermal network models

The thermal network models of the two system configurations can be used to calculate the thermal states of the primary and secondary circulation loops, the building envelope, the building internal space, the storage devices, and heat emitters at any point in time for a given set of boundary conditions (ambient temperature, irradiance, solar and internal gains), initial conditions (storage state of charge, space and

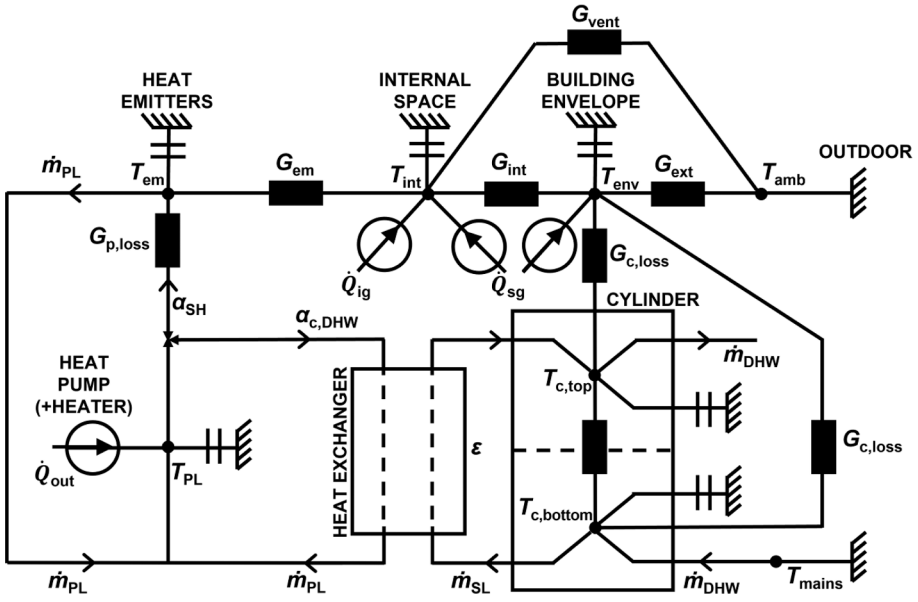

Fig. 4. Thermal network of standard configuration featuring the heat pump and auxiliary heater coupled with the heat emitters and DHW storage cylinder.

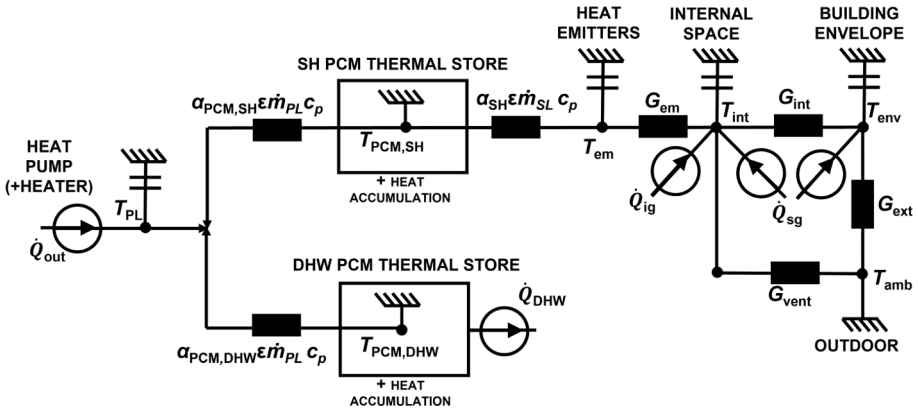

Fig. 5. Thermal network of advanced configuration featuring the heat pump and auxiliary heater coupled with two separate PCM thermal stores for SH and DHW. The heat exchangers and the losses from the two PCM thermal stores are not shown for simplification.

building envelope temperature), control strategy (heat pump and electric heater operation, valve control) and DHW demand.

2.2.1. Standard configuration with hot-water cylinder

The thermal network of the first configuration is based on a two-temperature stratified cylinder model and is shown in Fig. 4. The heat pump and auxiliary electric heater are coupled with the heat emitters and a heat exchanger transfers heat to the hot-water cylinder. A three-way valve is used to direct or shut off the heat-transfer fluid flow at the exhaust of the heat pump.

The heat exchanger is represented using a simple fixed effectiveness method, where effectiveness ε is the ratio of the actual and the maximum possible heat transfer. Furthermore, the three-way valve is modelled with the use of two binary variables: $\alpha_{c,DHW}$ and α_{SH}, which are equal to 1 when charging the hot-water cylinder or providing SH, respectively, and are equal to 0 when the system is turned off. At any point in time, only one of the two variables can be equal to 1. The circulation pump can keep running even when the heat pump and electric heater are switched off (i.e., $\alpha_{c,DHW}$ and α_{SH} can be equal to 1 even when the heat output from the heat pump and electric heater, $\dot{Q}_{out}$, is 0). Equations (1) - (8) correspond to the main structure of the thermal network shown in Fig. 4.

The rates of change of the temperature of the primary loop, the heat emitters, the internal space of the house and the building envelope are represented by Equations (1), (2), (3) and (4), respectively:

$$C_{PL}\frac{dT_{PL}}{dt} = \alpha_{c,DHW}\varepsilon\left(\dot{m}c_{p_w}\right)_{min}\left(T_{c,bottom} - T_{PL}\right) + \alpha_{SH}G_{p,loss}\left(T_{em} - T_{PL}\right) + \dot{Q}_{out}\,, \tag{1}$$

$$C_{em}\frac{dT_{em}}{dt} = \alpha_{SH}G_{p,loss}\left(T_{PL} - T_{em}\right) + G_{em}\left(T_{int} - T_{em}\right), \tag{2}$$

$$C_{int}\frac{dT_{int}}{dt} = G_{em}\left(T_{em} - T_{int}\right) + G_{int}\left(T_{env} - T_{int}\right) + G_{vent}\left(T_{amb} - T_{int}\right) + \dot{Q}_{ig} + \dot{Q}_{sg}\,, \tag{3}$$

$$C_{env}\frac{dT_{env}}{dt} = G_{int}\left(T_{int} - T_{env}\right) + G_{ext}\left(T_{amb} - T_{env}\right) + \frac{H_{c,bottom}}{H_{c,top}}G_{c,loss}\left(T_{c,bottom} - T_{env}\right) + \left(1 - \frac{H_{c,bottom}}{H_{c,top}}\right)G_{c,loss}\left(T_{c,top} - T_{env}\right) + \dot{Q}_{sg}\,, \tag{4}$$

where $\left(\dot{m}c_{p_w}\right)_{min}$ refers to the minimum capacity rate between those of the primary heat transfer fluid loop and the secondary DHW loop. The lumped heat capacity of the internal space represents both the internal air volume and furnishings. It is assumed that the cylinder is placed close to the building envelope and therefore any heat lost from the former enters the latter. The heights of the bottom (cold) and top (hot) sections of the cylinder depend on the mass of water in each section, although the total mass contained within the cylinder remains constant. These are in turn determined based on the flow rates of the hot water being provided by the heat pump and electric heater and the DHW demand:

$$\frac{dm_{top}}{dt} = \alpha_{c,DHW}\dot{m}_{SL} - \dot{m}_{d,DHW}\,, \tag{5}$$

$$\frac{dm_{bottom}}{dt} = \dot{m}_{d,DHW} - \alpha_{c,DHW}\dot{m}_{SL}\,. \tag{6}$$

Lastly, the rate of temperature change in the top and bottom sections of the cylinder is determined based on the heat transferred from the heat pump and electric heater through the heat exchanger, the DHW demand and the heat transferred through the thermocline (thin layer of abrupt temperature change that separates the upper and lower sections):

$$m_{top}c_{p_w}\frac{dT_{c,top}}{dt} = \alpha_{c,DHW}\left[\dot{m}_{SL}c_{p_w}\left(T_{c,bottom} - T_{c,top}\right) + \varepsilon\left(\dot{m}c_{p_w}\right)_{min}\left(T_{PL} - T_{c,bottom}\right)\right] + \frac{2\lambda_w\pi{R_c}^2}{H_c}\left(T_{c,bottom} - T_{c,top}\right), \tag{7}$$

$$m_{bottom}c_{p_w}\frac{dT_{c,bottom}}{dt} = \dot{m}_{d,DHW}c_{p_w}\left(T_{mains} - T_{c,bottom}\right) + \frac{2\lambda_w\pi{R_t}^2}{H_c}\left(T_{c,top} - T_{c,bottom}\right). \tag{8}$$

2.2.2. Advanced configuration with two PCM thermal stores

The thermal network of the second configuration shown in Fig. 5 is based on two PCM thermal stores, where one is used for SH and the other is used for DHW. The heat pump and auxiliary electric heater are coupled with the thermal stores and a three-way valve is again used to direct or shut off the heat-transfer fluid flow at the outlet of the heat pump. Thermophysical property values used to model the PCM thermal stores are based on a commercially available PCM product with a melting temperature of 48 °C [51], which is deemed appropriate for the dwelling considered in this work, where heat emitters are modern radiators. It should be noted, however, that a PCM with a lower melting temperature could be selected for dwellings with underfloor heating (typically down to 35 °C for a well-designed and well-insulated dwelling [52]), which would reduce the required heat pump delivery temperature and thus improve the overall performance. Further information is listed in Table A1 in the Appendix.

In this configuration, the three-way valve is modelled with the binary variables $\alpha_{PCM,DHW}$ and $\alpha_{PCM,SH}$, which are equal to 1 when charging the DHW PCM thermal store and SH PCM thermal store, respectively, and are equal to 0 when the system is turned off. Only one of the stores can be charged at any point in time. The binary variable α_{SH} determines when SH is provided depending on the thermostat command. The thermal network is represented by Equations (9) to (14).

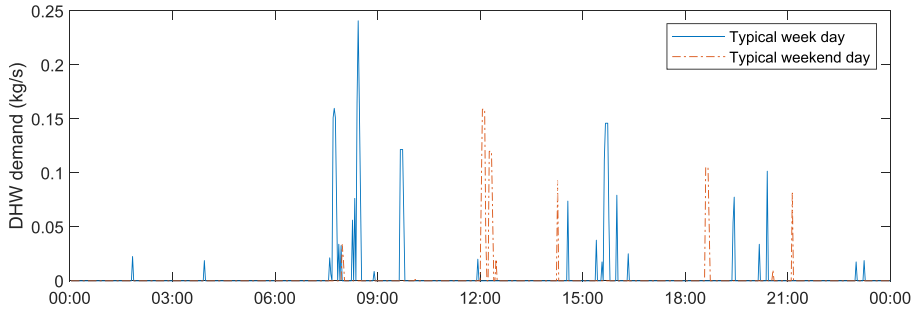

Fig. 6. Typical weekday and weekend day selected from the single-week probabilistic demand profile for domestic hot water. This represents a 3-bedroom / 4-person household.

The rates of change of the temperature of the primary loop, the heat emitters, the internal space and the building envelope are represented by Equations (9), (10), (11) and (12), respectively:

$$C_{\mathrm{PL}}\frac{\mathrm{d}T_{\mathrm{PL}}}{\mathrm{d}t} = \alpha_{\mathrm{PCM,DHW}}\varepsilon\dot{m}_{\mathrm{PL}}c_{\mathrm{p_w}}\left(T_{\mathrm{PCM,DHW}} - T_{\mathrm{PL}}\right) + \alpha_{\mathrm{PCM,SH}}\varepsilon\dot{m}_{\mathrm{PL}}c_{\mathrm{p_w}}\left(T_{\mathrm{PCM,SH}} - T_{\mathrm{PL}}\right) + \dot{Q}_{\mathrm{out}}\,, \tag{9}$$

$$C_{\mathrm{em}}\frac{\mathrm{d}T_{\mathrm{em}}}{\mathrm{d}t} = \alpha_{\mathrm{SH}}\varepsilon\dot{m}_{\mathrm{SL}}c_{\mathrm{p_w}}\left(T_{\mathrm{PCM,SH}} - T_{\mathrm{em}}\right) + G_{\mathrm{em}}\left(T_{\mathrm{int}} - T_{\mathrm{em}}\right) \tag{10}$$

$$C_{\mathrm{int}}\frac{\mathrm{d}T_{\mathrm{int}}}{\mathrm{d}t} = G_{\mathrm{em}}\left(T_{\mathrm{em}} - T_{\mathrm{int}}\right) + G_{\mathrm{int}}\left(T_{\mathrm{env}} - T_{\mathrm{int}}\right) + G_{\mathrm{vent}}\left(T_{\mathrm{amb}} - T_{\mathrm{int}}\right) + \dot{Q}_{\mathrm{ig}} + \dot{Q}_{\mathrm{sg}}\,, \tag{11}$$

$$C_{\mathrm{env}}\frac{\mathrm{d}T_{\mathrm{env}}}{\mathrm{d}t} = G_{\mathrm{int}}\left(T_{\mathrm{int}} - T_{\mathrm{env}}\right) + G_{\mathrm{ext}}\left(T_{\mathrm{amb}} - T_{\mathrm{env}}\right) + G_{\mathrm{PCM,SH,loss}}\left(T_{\mathrm{PCM,SH}} - T_{\mathrm{env}}\right) + G_{\mathrm{PCM,DHW,loss}}\left(T_{\mathrm{PCM,DHW}} - T_{\mathrm{env}}\right) + \dot{Q}_{\mathrm{sg}}\,, \tag{12}$$

where α_{SH} is a variable equal to 1 when SH is being provided and 0 when SH is not provided.

Lastly, the state of charge of the two PCM thermal stores is determined by the mass fraction (where $x = 1$ and $x = 0$ correspond to a full and empty store, respectively). The rates of change of the mass fraction of the DHW and SH PCM thermal stores are represented by Equations (13) and (14), respectively.

$$m_{\mathrm{PCM,DHW}}h_{\mathrm{L}}\frac{\mathrm{d}x_{\mathrm{PCM,DHW}}}{\mathrm{d}t} = \alpha_{\mathrm{PCM,DHW}}\varepsilon\dot{m}_{\mathrm{PL}}c_{\mathrm{p_w}}\left(T_{\mathrm{PL}} - T_{\mathrm{PCM,DHW}}\right) - \dot{m}_{\mathrm{d,DHW}}c_{\mathrm{p_w}}\left(T_{\mathrm{d}} - T_{\mathrm{mains}}\right), \tag{13}$$

$$m_{\mathrm{PCM,SH}}h_{\mathrm{L}}\frac{\mathrm{d}x_{\mathrm{PCM,SH}}}{\mathrm{d}t} = \alpha_{\mathrm{PCM,SH}}\varepsilon\dot{m}_{\mathrm{PL}}c_{\mathrm{p_w}}\left(T_{\mathrm{PL}} - T_{\mathrm{PCM,SH}}\right) + \alpha_{\mathrm{SH}}\varepsilon\dot{m}_{\mathrm{SL}}c_{\mathrm{p_w}}\left(T_{\mathrm{em}} - T_{\mathrm{PCM,SH}}\right). \tag{14}$$

2.3. Objective functions

The objective functions that represent the maximisation of energy bill savings (minimisation of operational cost) Obj_{cost}, average system COP $Obj_{\mathrm{COP_{sys}}}$ and self-sufficiency Obj_{suff}, are shown in Equations (15) - (17), respectively:

$$Obj_{\mathrm{cost}} = \min\sum_{t}\left(P_{\mathrm{elec}}(t) \bullet \dot{W}_{\mathrm{imp}}(t)\right), \tag{15}$$

$$Obj_{\mathrm{COP_{sys}}} = \max\sum_{t}\left(\dot{Q}_{\mathrm{out}}(t)\right) \Big/ \sum_{t}\left(\dot{W}_{\mathrm{in}}(t)\right). \tag{16}$$

$$Obj_{\mathrm{suff}} = \min\sum_{t}\left(\dot{W}_{\mathrm{imp}}(t)\right) \Big/ \sum_{t}\left(\dot{W}_{\mathrm{in}}(t)\right), \tag{17}$$

In the above equations, P_{elec} refers to the time-resolved price per unit of imported electricity; $\dot{W}_{\mathrm{imp}}$ the time-resolved imported electricity; $\mathrm{COP_{sys}}$ the average system COP (ratio of the sum of the heat output to the sum of the electricity consumption of the heat pump and auxiliary electric heater); $\dot{W}_{\mathrm{imp}}$ the time-resolved imported electricity; and $\dot{W}_{\mathrm{in}}$ the time-resolved electricity consumption.

2.4. Main inputs and assumptions

All modelling work was developed using object-oriented programming in MATLAB [53]. The thermal conductance and capacitance values used to represent the house are based on a modern, detached, 3-bedroom residential dwelling in the UK [54] and are provided in Table A2 in the Appendix. These values are assumed to be the same for both the UK and German locations in order to simplify the analysis. However, it is acknowledged that there is a significant difference in insulation standards and construction types between the two countries. For German homes, insulation levels generally tend to be higher than in the UK and wall insulation is more commonly applied to the external rather than the internal surface. Therefore, it is likely that several German homes could make further use of the thermal inertia of the dwelling itself compared to what is shown in this work.

2.4.1. Heat demand

The DHW demand is based on a single-week probabilistic demand profile and the reference supply temperature is 43 °C, which is in the typical range for bath, shower and most other domestic hot-water applications [55,56]. Whenever water is available at a higher temperature, it is assumed to be mixed down with mains water at 10 °C. The DHW usage profiles were generated using the "DHWCalc" tool developed by the University of Kassel [57]. A full year of consumption data were generated at 2-minute resolution and calibrated to represent a three-bedroom / four-person household. The single-week profile was selected to be the most representative of the average week. A typical weekday and weekend day are shown in Fig. 6.

The SH demand is based on the temperature of the internal space of the house. For both configurations, SH is provided using a thermostat to switch on the heating system whenever the internal space temperature falls below 18 °C and switch off whenever the internal space temperature rises above 22 °C (18 °C is recommended by Public Health England for comfort and minimising health risks in winter [58]).

At any point in time, the heating system can only provide heat for DHW or SH. Even when the operation is optimised, depending on the size of the system components and the operating conditions, it is sometimes not possible to meet all required demand. In all simulations using the first configuration, if both charging the hot-water cylinder and SH are required at the same time, priority is always given to charging the

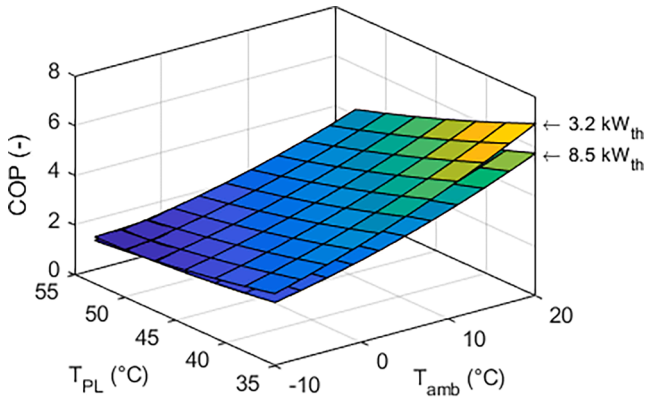

Fig. 7. COP as a function of the ambient temperature T_{amb} and the temperature of the primary loop (supply temperature) T_{PL} for the nominal heating capacity of 8.5 kW_{th} and the minimum heating capacity of 3.2 kW_{th}.

hot-water cylinder. Similarly, in the second configuration, if both the DHW and SH thermal stores require charging at the same time, priority is given to the former.

In the developed model, if there is demand for DHW and the temperature of the top of the cylinder is below the minimum threshold value of 43 °C, or there is not enough hot water, the DHW demand is considered "not met". Similarly, if the internal space temperature falls below 16 °C (either because SH demand is very high or because the DHW is being given priority, the SH demand is considered "not met"). When demand is not met, a penalty is added to the operational cost and system COP at a later stage, which corresponds to supplying the demand using an electric heater (i.e., with a COP of 1).

2.4.2. Technologies

The ASHP considered in this study has a nominal heating capacity of 8.5 kW_{th}, and the COP is modelled as a function of the heating capacity and temperature lift (supplied flow temperature minus outdoor ambient temperature) using a performance map generated from tabulated operational data [48]. The feasible operating region applied in the performance map is based on the ambient temperature, flow temperature and output capacity limits defined in the tabulated data.

The performance map generated from the heat pump data is shown in Fig. 7. The two 3-D surface plots represent the COP at two different heating output capacity levels: 8.5 kW_{th}, representing the nominal heat pump output; and 3.2 kW_{th}, representing the minimum feasible output applied in the performance map. The performance at any intermediate output level lies within the region bounded by the two surfaces. It is noted that the heat pump COP is found to increase slightly as output capacity is reduced.

It is noted that in cold-weather conditions, ASHPs can experience frost formation on the evaporator surface that inhibits heat transfer and impacts overall performance in heating mode. Thus, most ASHP systems incorporate an automatic defrost cycle into their operation. In this work, a detailed dynamic model of the heat pump frosting and defrosting behaviour is not included as part of the optimisation. However, the tabulated data used to derive the heat pump performance curve used does include the parasitic energy consumption that would result from periodic defrosting at low ambient temperatures, as specified by European Standard EN 14511 [59].

The backup electric heater is modelled with a fixed output of 3 kW_{th} and is operated only when heating demand exceeds the nominal heat pump output or environmental conditions are outside of the feasible operating region of the performance map.

The solar-PV array properties are based on the datasheet specifications of a commercially available mono-crystalline module [60]. Each panel has a nominal electrical efficiency of 17.4 % and a temperature coefficient of −0.39 %/K. The total array size is based on 8 panels with a combined area of 13 m^2. The panel inclination is assumed to be 30° from horizontal, in line with the optimal tilt angle used in the UK [61] and the inverter efficiency is equal to 96 % [62].

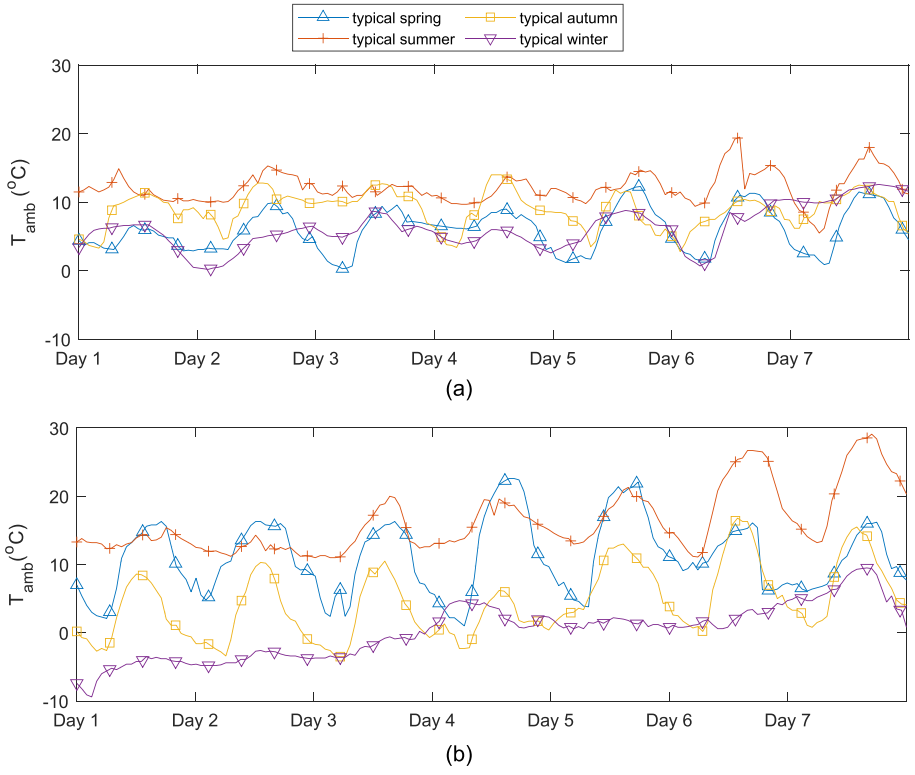

Fig. 8. Ambient temperature for four selected weeks in (a) Oban, UK; and (b) Munich, Germany.

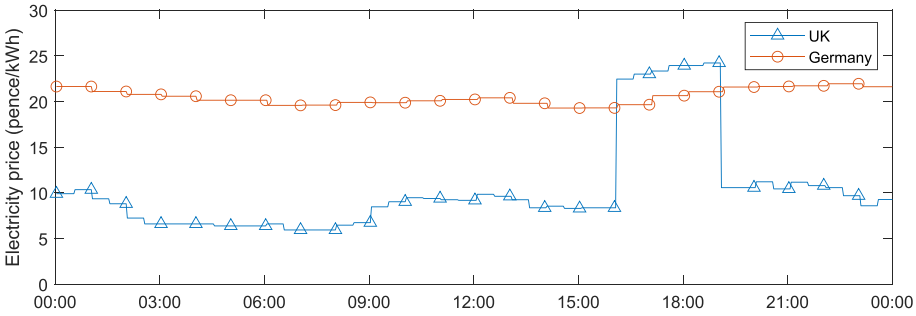

Fig. 9. Typical daily profile of time-of-use electricity price for (a) UK; and (b) Germany.

2.4.3. Weather data and selected weeks for UK and Germany

The weather data source used for this study was the International Weather for Energy Calculations published by ASHRAE [63]. Ten weather data locations were analysed for the UK and continental Europe on the basis of temperature, solar irradiance and heating degree days. Oban in Scotland, UK, was chosen to represent a climate region with mild summers and winters and a moderate solar yield, while Munich in Southern Germany was chosen to represent a more extreme climate region with hot summers, cold winters, and a higher annual solar yield. For the analysis, four typical weather weeks are extracted from the annual data sets for each season, nearest the average temperatures of each season. Ambient temperatures for the two locations are presented in Fig. 8.

2.4.4. Electricity tariffs for the UK and Germany

Historic electricity price data from the year 2019 was selected for the analysis, based on the most popular dynamic time-of-use tariffs currently available in the UK and Germany. These tariffs allow end-users to benefit financially by shifting their electricity use to a time of day when electricity price is low. For the UK, the Octopus Agile tariff was selected; this tariff exhibits a peak price period between the hours of 16:00–19:00, while unit charge is updated each day based on wholesale price [64]. For Germany, the aWATTar tariff was selected; this tariff is based on the EPEX Spot DE price plus an additional 20c/kWh for tax and grid usage charges [65]. Electricity price variation for the two tariffs over a typical 24-hour period are presented in Fig. 9, converted to Pound Sterling (GBP). It can be observed that the aWATTar (German) tariff typically exhibits a smaller daily variation in unit price and does not exhibit the characteristic early-evening price peak of the Octopus Agile (UK) tariff. Furthermore, the average unit price is generally higher for the former due to the higher tax and other fixed unit charges in Germany. Standing charge is not included, as this does not depend on electricity demand and does not affect the heat pump operation, nor the projected operational cost savings.

2.4.5. Irradiance and solar-PV system calculations

The PV system output is calculated based on the weather, day of the year, time, location, panel inclination and panel orientation. Solar irradiance incidence-angle calculations are performed using the calculation procedure summarised in Kalogirou [66]. The total irradiance incident on the tilted surface of the PV panel is equal to the sum of the beam, diffuse and ground-reflected components and is calculated using the model developed by Reindl et al. [67].The cell temperature is determined using the methodology by HOMER Energy [68] and the PV system power output $\dot{W}_{PV}$ is estimated using:

$$\dot{W}_{PV} = n_{pan}\eta_{inv}\eta_{nom}\left[1+\gamma\left(T_{pan}-298.15\right)\right]I_{gt}A_{pan}\,. \tag{18}$$

2.5. Simulated baseline and optimisation cases

All simulations assume that weather, price and demand forecasts are known with perfect accuracy. Nonetheless, the optimisation cases can be used to assess the maximum potential of smart control strategies based on forecast data and to identify favourable periods for charging and discharging the thermal storage in comparison to the baseline case.

2.5.1. Baseline case

Identifying the potential of smart heat pump operation strategies requires the comparison of the obtained results to a baseline case based on a standard configuration. Most studies in the literature compare the costs associated with an optimised heat-pump operation to a baseline case based on traditional gas or oil boilers [26,29,30]. The downside of this approach is that any observed economic or performance improvements could be attributed to the change of technology itself or the assumptions regarding the difference in prices for the alternative fuel sources. In this work, the baseline case considers the same technology configuration as the first optimisation case: a heat pump with a nominal capacity of 8.5 kW_{th} coupled with a hot-water cylinder (Fig. 2 in Section 2.1). This allows an assessment of whether benefits can be achieved by using a smart control strategy or a different storage configuration. The hot-water cylinder is assumed to have a volume of 200 L, which is typical for a four-person household [33]. The initial state of charge of the cylinder is set to 50 % for all simulations, meaning that some hot water is already available at the beginning of the time horizon in case there is early demand.

The simplified control strategy used in this baseline case is as follows: the charging of the hot-water cylinder is activated whenever the temperature of the water at the top or bottom of the cylinder falls below the minimum threshold value (43 °C) and is deactivated whenever half of the water in the cylinder is above a maximum threshold value (50 °C).

In this baseline case, both DHW heating and SH involve the heat pump being operated at nominal capacity (i.e., typically ~ 8.5 kW_{th} at moderate outdoor temperatures). Since in this simplified strategy DHW heating is activated based on temperature sensors, the DHW cylinder cannot be used to time-shift the heat pump operation. The simulation timestep is set to 2 min.

2.5.2. Optimisation cases

In Optimisation Case 1, the standard configuration of a heat pump coupled with a hot-water cylinder is investigated but this time the operation is optimised with respect to the objective functions of Equations (15) - (17). The heat pump and hot-water cylinder have the same size and as the baseline case: 8.5 kW_{th} and 200 L, respectively. The decision variables include the binary decision of whether the cylinder should be charged $\alpha_{c,DHW}$ and the heat required by the heat pump and electric heater $\dot{Q}_{out}$. The heat-pump maximum operating temperature is 60 °C and therefore the primary loop temperature rarely reaches higher values. A higher value is used as a constraint for the optimiser (70 °C) to provide flexibility, by allowing the use of the electric heater at those temperatures if demand is very high.

Optimisation Case 2 involves the advanced configuration with the two PCM thermal stores: one to store thermal energy for DHW heating and one to store thermal energy for SH. The analysis aims to explore the

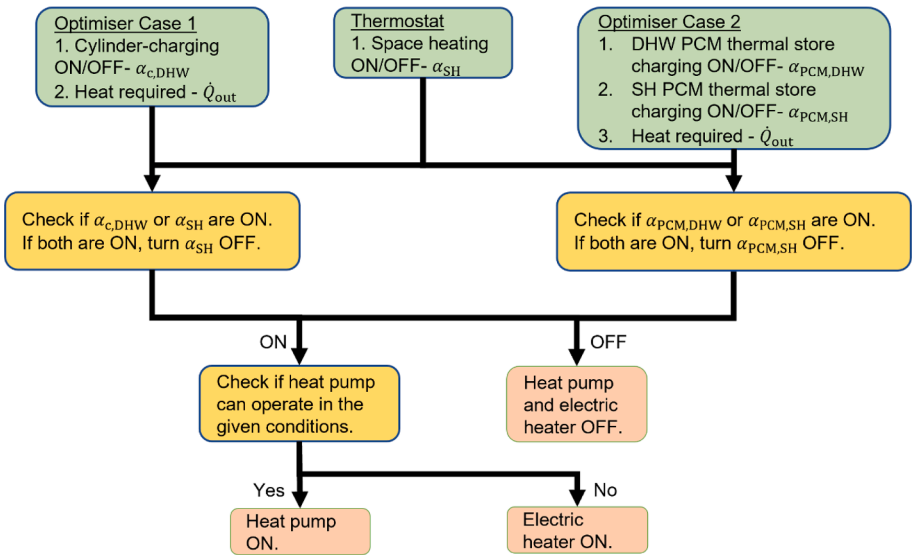

Fig. 10. Control strategy framework for the optimised standard configuration of an ASHP coupled with a hot-water cylinder and the advanced configuration of an ASHP coupled with two PCM thermal stores.

potential for even further economic and energy-efficiency gains, using smart control in conjunction with a more advanced system configuration. Again, the operation is optimised with respect to the objective functions of Equations (15) - (17). The decision variables include the binary decision of when to charge the DHW PCM thermal store $\alpha_{PCM,DHW}$, the heat required by the heat pump and electric heater $\dot{Q}_{out}$, as well as an additional binary decision determining when to charge the SH PCM thermal store $\alpha_{PCM,SH}$. The temperature for the primary loop is constrained to be lower than 60 °C. The control strategy framework for both optimisation cases is presented in Fig. 10.

In all optimisation simulations, a modified part-load model of the heat pump operation is implemented to provide greater operation flexibility compared to the baseline case. This allows the heat pump to be operated at a capacity lower than the nominal capacity when this is beneficial. The controller temporal resolution (amount of time after which the decision variables change) is set to 30 min. However, the thermal state of the system is calculated every 2 min (similar to the baseline case); if it is impossible to implement a new operating state for the whole 30 min, the latter is adjusted accordingly. The initial state of charge is set to be the same as the baseline case and the cylinder or PCM thermal stores can be charged further straight away if that is found to be beneficial.

3. Results

This section presents the results of the operational optimisation of: (i) the standard configuration of an ASHP coupled with a DHW cylinder; and (ii) an advanced configuration of an ASHP coupled with two PCM thermal stores for SH and DHW. The developed optimisation problems are constrained MINLPs. In order to solve these, a genetic algorithm methodology is employed, which involves a population of possible solutions to repeatedly update and improve until an optimal solution is obtained. For all simulations, the time horizon is set to 1 week. The Global Optimisation Toolbox of MATLAB [53] is used. The initial population size, the function tolerance and the constraint tolerance are set to 200, 0.001 and 0.001, respectively. The crossover fraction, which controls how "parent" individuals combine to form "children" individuals for every generation, is set to 0.8. The default mutation option of the toolbox is used, which adds a mutation chosen from a Gaussian distribution to each entry of the parent vector. The amount of mutation decreases for every new generation. The maximum number of generations is set to be 100 times larger than the number of optimisation variables in each optimisation case.

Table 1
Summary of baseline case results for the typical weather weeks in each season for the UK location.

Selected week	Operational cost (£/day)	Average system COP (-)	Self-sufficiency (%)	Electricity consumption (kWh/day)
Typical spring	1.30	2.39	8.96	14.4
Typical summer	0.50	2.81	16.41	5.60
Typical autumn	1.06	2.58	3.94	11.1
Typical winter	1.61	2.42	3.88	15.9

Table 2
Summary of baseline case results for the typical weather weeks in each season for the German location.

Selected week	Operational cost (£/day)	Average system COP (-)	Self-sufficiency (%)	Electricity consumption (kWh/day)
Typical spring	1.40	2.66	12.24	7.20
Typical summer	0.90	3.11	18.20	4.60
Typical autumn	3.63	2.31	8.11	17.9
Typical winter	5.83	2.18	1.49	27.2

3.1. Baseline case: Standard configuration with hot-water cylinder

The baseline results are provided in Tables 1 and 2. The operational cost and the electricity consumption are provided as daily quantities.

As shown in Tables 1 and 2, the system performance and operational cost over a typical year varies significantly according to the location and seasonal climate. For example, the operational cost in the UK location, which experiences milder seasonal climate variations, is approximately 3 times higher for the typical winter week than for the typical summer week. In the German location, which has a more extreme climate, the

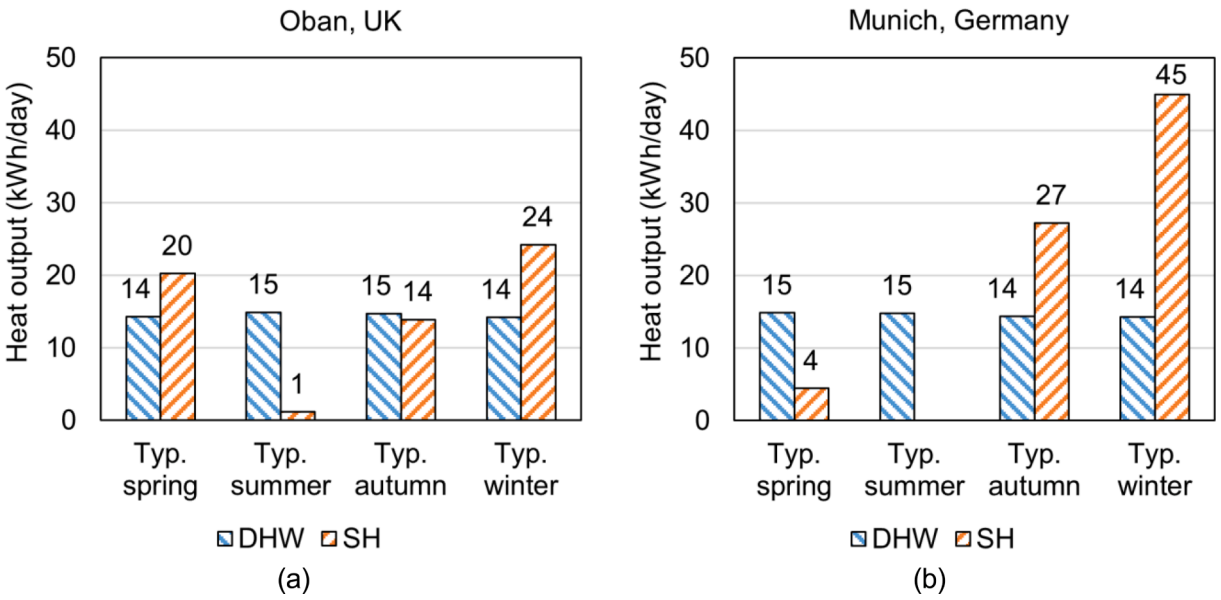

Fig. 11. Daily heat pump heat outputs for each simulation week in (a) Oban, UK; and (b) Munich, Germany. Results for DHW and SH are shown in separate bars.

operational cost is more than 6 times higher for winter than for summer. Similarly, for the German location the degree of seasonal variation in system COP is more than twice that of the UK location.

The role of the backup electric heater in the baseline case is minimal for all simulated weeks. Backup heaters are typically included as redundancy to prevent excessive oversizing of the heat pump for extreme winter conditions. As shown in Tables 1 and 2, depending on the location and time of the year, the heater only covers 0–2 % of the total heat demand. It is only operated when the conditions are outside the feasible operating range of the heat pump.

Fig. 11 presents the total heat output for the provision of DHW and SH for the baseline case in the two locations. The heat pump system produces a relatively constant 14–15 kWh/day to provide DHW demand across all seasons. For SH however, the required thermal output to meet the demand largely depends on the location and season. In the UK case, the heat output required for SH varies between 1 and 24 kWh/day for the selected weeks, while for the German case, which features lower outdoor temperatures during autumn and winter, it varies between 0 and 45 kWh/day. In both locations, SH requirements during a typical summer week are minimal.

For all simulated periods in the baseline case, the DHW demand is mostly met within the defined constraints of the optimisation problem. For a very small fraction of the time (0.6 % for the UK case and 1.1 % for the German case) it was not possible for the simulated system to meet the peak DHW load, and DHW supply temperature briefly drops below the minimum specified 43 °C.

3.2. *Optimised Case 1: Standard configuration with domestic hot water cylinder*

Results for Optimised Case 1 are presented in Fig. 12 and compared to the baseline case results for the four typical weather weeks. In Fig. 13, the results are aggregated to demonstrate the annual-average values for each objective function.

An analysis of Figs. 12 and 13 reveals that optimising the operation of a domestic ASHP can lead to significant improvements in all three objectives relative to the baseline, regardless of which objective function is chosen for the optimisation. In all simulations, less than 1 % of demand is not met at the time requested and less than 0.1 % of the demand is provided by the backup electric heater.

When the objective function is the operational cost, an average annual cost saving of 22 % (0.24 £/day) is obtained for the UK case and 20 % (0.57 £/day) is obtained for the German case (Fig. 13(a)). Even in periods of low SH demand, (e.g., summer, Fig. 12(a) and Fig. 12(b)), costs can be reduced in both locations. This is attributed to the fact that heating of the DHW storage cylinder can be used to shift a significant fraction of heat pump operation away from high electricity-price periods. Cost savings are also obtained with the other two objective functions, albeit to a lesser extent. Applying COP maximisation as the objective function results in overall cost savings of 13 % in the UK case and 17 % in the German case; while the self-sufficiency maximisation objective results in an 18 % cost reduction for both locations.

Using the average system COP as the objective function leads to a COP increase of 7 % in UK case and 9 % in the German case (Fig. 13(b)). This is a result of shifting the DHW heating process towards high ambient-temperature periods and minimising the use of the backup electric heater, which is only activated when it is not possible to meet the demand with the heat pump alone.

When self-sufficiency maximisation is applied as the objective function, a significant increase in the overall self-sufficiency fraction is observed for all simulated weather weeks. This is achieved by charging the DHW cylinder as much as possible when local electricity generation is available from the PV array. In the UK case for example, self-sufficiency is increased from 16 % to 36 % in the typical summer week and from 4 % to 15 % in the typical autumn week. For the annual-averaged results in Fig. 13(c), the overall optimised self-sufficiency fraction is approximately double the baseline case for both locations.

Important conclusions can be drawn from the comparison of the optimised results using the three different objective functions. First, the use of any of the objective functions leads to a simultaneous improvement in the other two objective functions. This is an important result as it means that end-users could choose any of these three objective functions with the knowledge that they are not causing deterioration in other important objectives. Another interesting conclusion is that in many cases, the three objectives perform equally well, meaning that the objective function is minimised or maximised at the expense of only small reductions in the potential of the other objectives. For example, in the German case, the COP improvement when the objective function is the operational cost or self-sufficiency in is almost the same as when the system COP is used as the objective function (7–8 %, see Fig. 13(b)). One exception to this is the significant difference in operational cost in the UK case when the objective function is changed from operational cost to system COP. In this case, the electricity price tariff exhibits a large increase in unit price between the peak hours of 16:00–19:00 (see Fig. 9).

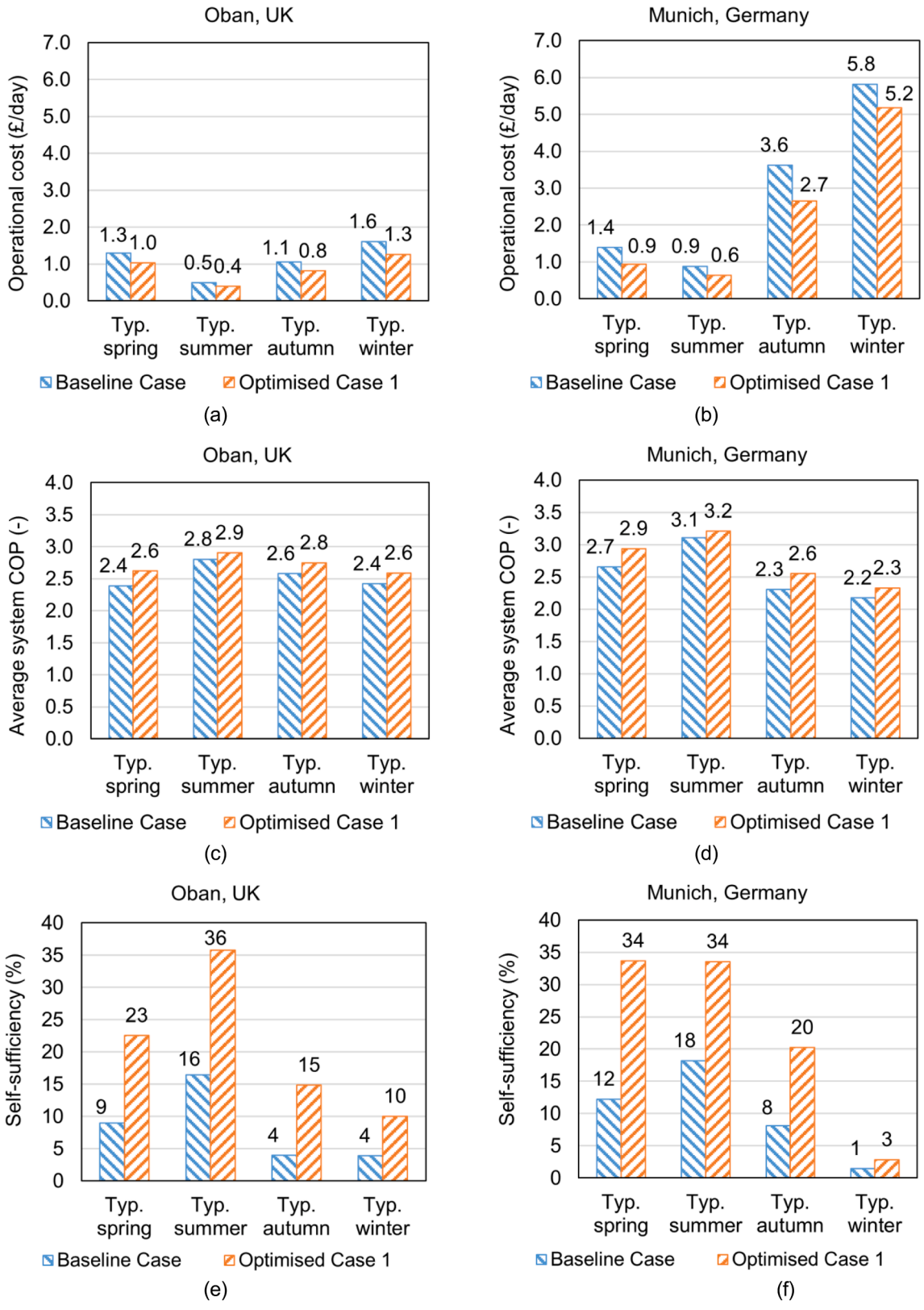

Fig. 12. Results for the optimised standard configuration with a hot water cylinder volume of 200 L. The objective function is the minimum operational cost for (a) and (b), the maximum average system COP for (c) and (d) and the maximum self-sufficiency for (e) and (f). The baseline case results are shown for comparison.

However, these hours are also the period of the day when outdoor ambient temperature is often warmest, and thus it is most favourable to operate the heat pump to charge the thermal storage when maximising the system COP. Thus, the maximum-COP optimisation seeks to shift heat pump usage towards these hours, while the minimum-cost optimisation seeks to shift heat pump operation away from these hours. The cost saving obtained using the maximum-COP objective function is therefore considerably lower. This is not observed to the same extent for

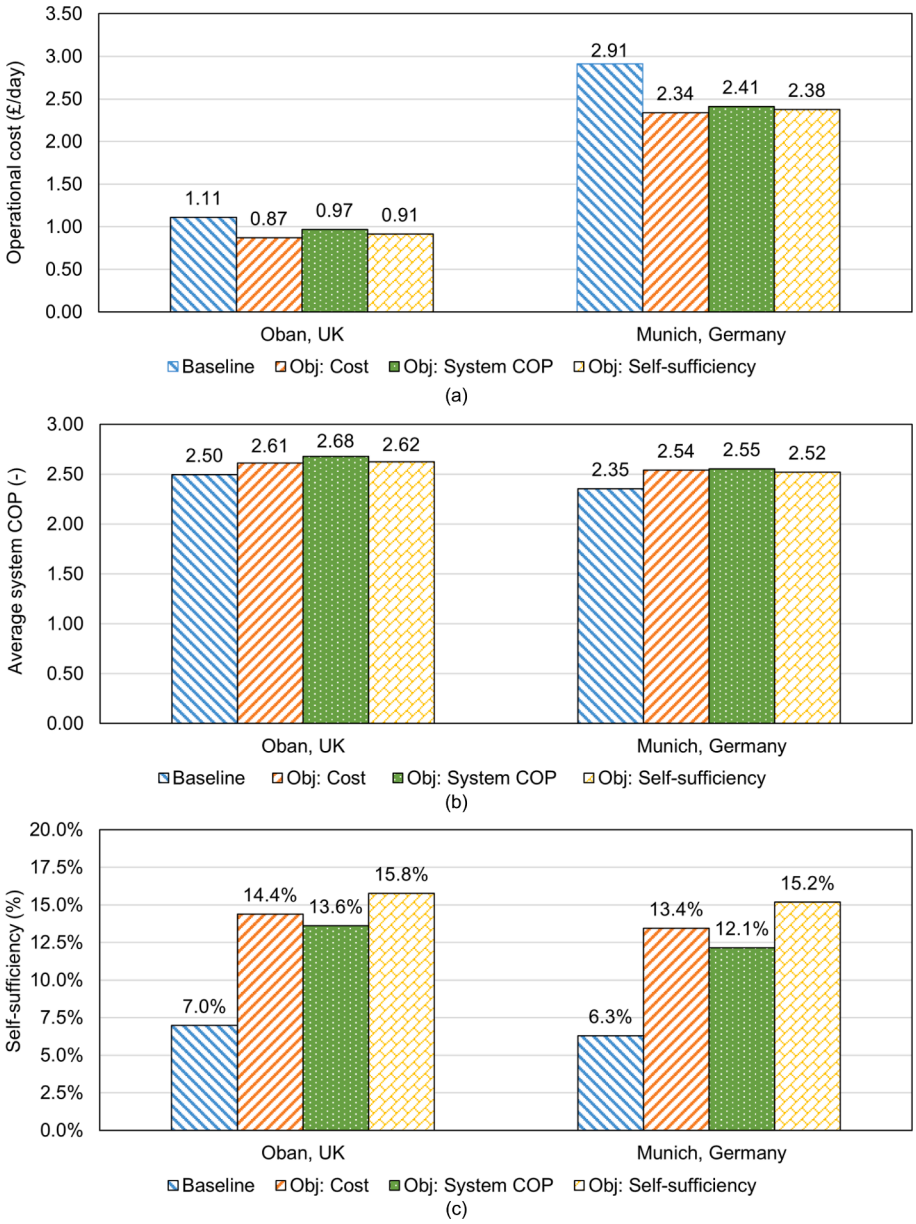

Fig. 13. Annual averages for the optimised 200-L hot water cylinder case when compared to the baseline case for: (a) operational cost; (b) system COP; and (c) self-sufficiency.

the German case, where the variable price tariff exhibits less price variation over the day and thus cost-saving potential is less dependent on avoiding peak price periods.

3.3. Optimised Case 2: Advanced configuration with DHW and SH thermal stores

The advanced configuration chosen for this optimisation case features separate PCM thermal stores for DHW and SH, as shown in Fig. 3. As PCM thermal stores are not widely available for domestic applications at present, there is not an established approach to sizing such storage systems (compared to, for example, BS EN 15450 [69] which covers DHW cylinder sizing for heat pumps applications). For the present study, a simplified sizing exercise was performed to select the volume of the two PCM thermal stores to be used in the rest of the analysis. The approach taken was to limit the total storage volume for the two stores to 200 L, which is the same overall volume as the DHW cylinder in the baseline case and is considered a reasonable storage volume for a typical small- or medium-sized house. The relative proportion split between the DHW and SH storage was then varied in 25 % intervals to examine the influence on selected cases from the optimisation study. The operational cost (Equation (15)), which is considered one of the most important performance indicators, was used as the objective function. The exercise was performed for the UK and German locations based on the typical winter weeks, which have the highest overall heating demand. The results are shown in Fig. 14, with cost saving for each sizing combination presented relative to baseline-case result.

Fig. 14 shows that the best performance in terms of operational cost reduction is achieved by applying a 50–50 % volume split between DHW thermal storage and SH thermal storage. The cost-saving potential decreases as the SH volume fraction is reduced below 100 L, demonstrating the additional operational flexibility associated with SH time-shifting in winter. However, due to the higher peak heating loads associated with the DHW demand, the DHW thermal storage has a minimum critical volume requirement in order to meet this demand. A smaller thermal

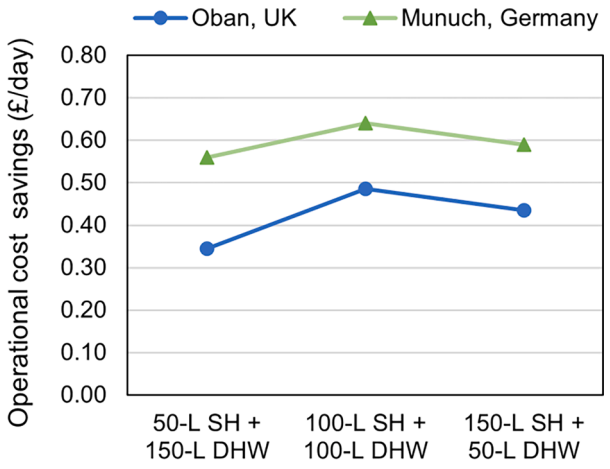

Fig. 14. Operational cost savings compared to the baseline case using operational cost as the objective function arising from three different PCM DHW and SH thermal storage volume combinations: (a) 50 L for SH and 150 L for DHW; (b) 100 L for SH and 100 L for DHW; and (c) 150 L for SH and 50 L for DHW.

storage volume for DHW also leads to limited flexibility during high electricity-price periods and to the electric heater being operated more often. Based on these results, a volume of 100 L was chosen for both the DHW and SH PCM thermal stores to be applied Optimisation Case 2.

Fig. 15 shows results for a 100-L SH thermal store and a 100-L DHW thermal store for each location, season, and objective function. The results are again aggregated to demonstrate the annual-average values of each performance indicator in Fig. 16. The analysis of Figs. 15 and 16 shows a greater reduction in operational cost compared to Optimised Case 1, indicating a higher potential for optimisation with the proposed PCM thermal storage configuration. As was also observed for Optimised Case 1, less than 1 % of the heat demand is not met at the time requested, and use of the electric heater is minimal.

For the operational cost objective function, the advanced system configuration with PCM thermal storage shows an improvement over the basic system configuration for both locations and all seasons. Although the inertia of the dwelling itself allowed for some flexibility in Optimised Case 1, the addition of the SH thermal store in Optimised Case 2 is shown to be highly influential, unlocking further potential for shifting the SH operation towards low electricity-price periods, while also satisfying heating demand within the space-temperature constraints. This contribution is most beneficial in during the mid-season periods, with operational cost savings of >30 % observed for both the UK and German locations. Absolute savings are lower in summer due to the minimal requirement for SH; while in winter the operational flexibility is restricted due to higher peak heating loads, particularly for the German location. When COP is set as the objective function, an overall COP improvement of 9 % is obtained for the UK case, compared to 5 % for the German case. For the latter location especially, the result is dominated by the winter period when the average SH load is close to the nominal thermal output capacity of the heat pump, thus limiting the potential to operate the heat pump flexibly with respect to time. For the advanced system configuration, the heat pump COP shows less variation with state of charge of the storage medium because the return temperature to the heat pump is approximately constant during melting of the PCM. On average the operating temperature of the heat pump is found to be slightly higher for the advanced configuration than for the standard configuration, and thus the COP improvement is negligible despite the increased storage capacity and increased potential for time-shifting of the heat pump operation.

Setting COP as the objective function also results in a trade-off between energy savings and running-cost savings, which is evidenced by the increase in operational cost shown for the COP objective (Fig. 16(b)) compared to the cost-saving objective (Fig. 16(a)). When comparing the two objective functions, the relative improvement in COP is smaller than the relative reduction in cost savings (particularly for the German case), which suggests that cost savings may be preferable to COP maximisation as an optimisation objective.

Lastly, when self-sufficiency is set as the objective function, Figs. 15 (e) and 15(f) shows that the fraction (in %) of heat pump energy demand covered by the PV system is increased more than 3-fold for all seasons. The operating schedule is optimised to convert most of the generated electricity from the PV system into stored heat for later use. Fig. 16(c) shows that when averaged over the four seasons, this results in 34 % of heat pump electrical demand covered for the UK location and 24 % covered for the German location (compared to 7 % and 6 % in the respective baseline cases). It is also observed that the self-sufficiency objective presents a better compromise between cost savings and energy savings compared to the other two objective functions. Specifically, the overall cost savings achieved with the self-sufficiency objective function are less than 10 % lower than that achieved with the cost-minimisation objective (summarised in Fig. 16(a)); while the average COP is less than 2 % lower than that achieved with the COP maximisation function (summarised in Fig. 16(b)).

It can thus be concluded that choosing any of the three objective functions improves the other two objectives relative to the baseline case. This is consistent with the results obtained from Optimisation Case 1. As described above, the use of the operational cost as the objective function minimises overall running cost but significantly reduces average system COP (particularly for the UK electricity price tariff), while the COP objective function maximises COP improvement, but significantly reduces cost savings. Optimising the system for self-sufficiency, on the other hand, comes at the expense of significantly smaller reductions in the other objectives and presents the best compromise between cost and energy savings. The amount of imported electricity is minimised, which leads to substantial improvements both in terms of cost and average system COP relative to the baseline.

3.4. Comparison of time-resolved results

This section presents time-resolved results for the three optimisation objectives investigated in this paper. In order to identify recurring patterns in the daily operation of the system, the heat pump and electric heater outputs for SH and DHW are provided as shaded area plots, overlaying the 7 days of the week. The typical autumn week in for the UK location is used as an example, since a significant improvement in all three objective functions was observed for this case with both system configurations.

The time-resolved operation in the baseline case is shown in Fig. 17. The simplified thermostatic control leads to the heat pump being switched on, in most cases, for significant periods of time in the morning hours (07:00–10:00). During these hours, the demand for SH is significant (Fig. 17(a)) due to the ambient temperature being relatively low compared to the rest of the day. The demand for DHW is also very high (Fig. 17(b), Fig. 6 in Section 2.4.1). A significant portion of the electricity produced by the solar-PV system is not used and is instead exported to the grid. This is demonstrated by the negative values of net energy exchange with the grid in Fig. 17(c). The internal space temperature is maintained around 20 °C within the dead-band of the thermostatic control (Fig. 17(d)). During DHW operation, whenever hot water is extracted from the top of the DHW cylinder, cold water simultaneously enters at the bottom. The drop in stored water temperature causes the heat pump to heat the water to the DHW storage set point temperature (Fig. 17(d)).

Time-resolved operation profiles for the three optimisation objectives with the standard DHW cylinder configuration (Optimised Case 1) are presented in Figs. 18 - 20. In Fig. 18, it is interesting to observe the times of SH and DHW heating with respect to the time-varying electricity price. Heating of the DHW cylinder often occurs in the morning, 08:00–12:00, or early afternoon, 15:00–16:00, avoiding the peak

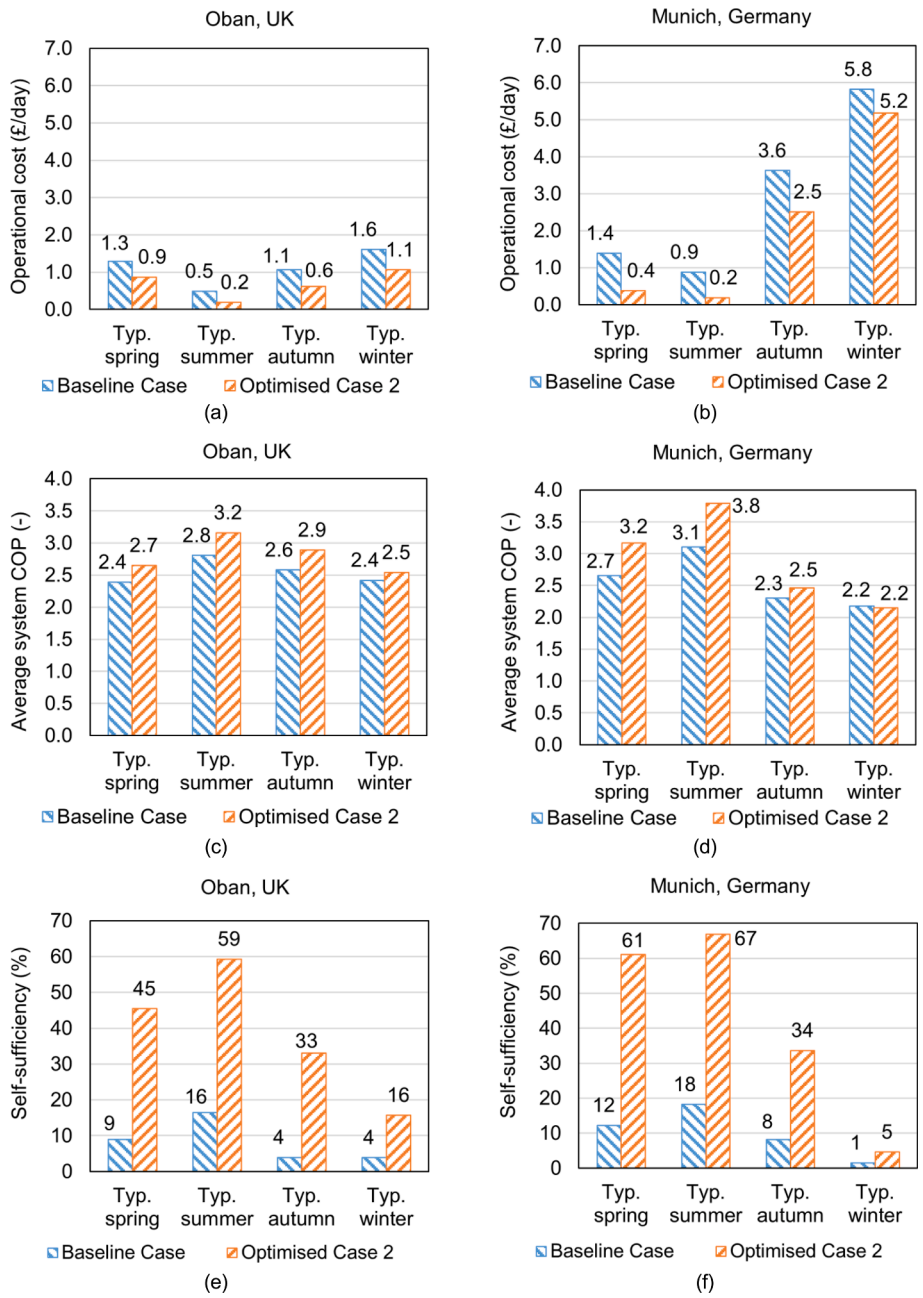

Fig. 15. Results for the optimised configuration with two PCM thermal stores (100 L for DHW and 100 L for SH). The objective function is the minimum operational cost for (a) and (b), the maximum average system COP for (c) and (d) and the maximum self-sufficiency for (e) and (f). The baseline case results are shown for comparison.

periods of the variable electricity price tariff occurring between 16:00 and 19:00 (Fig. 18(b)). Furthermore, although the standard configuration does not have a dedicated thermal store for SH, the optimiser takes advantage of the inertia of the dwelling itself and modulates the heat pump's output capacity in such a way that any SH requirements during high-electricity price periods are avoided. This is clearly illustrated in Fig. 18(a), which shows that SH is avoided between 16:00 and 19:00 for all days of the week.

A visual comparison of Figs. 18 and 19 illustrates that the operational profile for maximum COP is significantly different to that for minimum operational cost. Fig. 19(a) shows that to maximise COP, the heat pump is often operated at a lower, part-load capacity when providing SH. Although this leads to longer-duration periods of SH that sometimes coincide with high electricity-price periods, the average system COP is higher when the heat pump operates at reduced output (Fig. 7 in Section 2.4.2). Additionally, a higher portion of DHW heating also takes place during high ambient-temperature periods, between 12:00 and 15:00, compared to when optimising the operational cost (Fig. 19(b)).

When the objective function is self-sufficiency (Fig. 20), the heat pump is operated mostly during daylight hours, both in the case of SH (Fig. 20(a)) and DHW heating (Fig. 20(b)). The ability to adjust the provision of SH even without a dedicated SH store is again attributed to the house thermal inertia. This means that a large proportion of the electricity produced from the rooftop PV array can be used to power the heat pump; while the requirement for imported electricity is further reduced because ambient temperature and COP are higher, and thus overall electricity demand is lower.

Figs. 21-23 compare operational profiles for the three optimisation objectives applied to the advanced thermal storage configuration (Optimised Case 2), which uses separate PCM heat stores for DHW and

Fig. 16. Annual averages for the optimised cases with two PCM thermal stores (100 L for DHW and 100 L for SH) when compared to the baseline case for: (a) operational cost; (b) system COP; and (c) self-sufficiency.

SH. The main advantage of this configuration is that the second thermal store allows the SH demand to be almost fully decoupled temporally from the operation of the heat pump, while the overall thermal storage capacity of the system is increased due to the higher storage density of the PCM.

As shown in Fig. 21(a), when the objective function is the operational cost, the heat pump never charges the SH thermal store during peak electricity-price hours (16:00–19:00). Most often this occurs during early morning (03:00–05:00) or midday (10:00–15:00), when the SH demand is high and the price is low. Fig. 21(b) shows that the heat pump is also less frequently required to charge the DHW thermal store during peak-electricity price hours, when compared to the baseline case and the optimised case based on the standard configuration. This is attributed to the fact that the 100-L PCM thermal store has a higher energy storage capacity in the operating temperature range than the 200 L cylinder.

When the objective function is the average system COP, the heat pump is switched on as much as possible to charge the store when the ambient temperature is high. From Fig. 22(a) and (b), it can be concluded that although the SH demand is usually higher during the night, both thermal stores are mainly charged during the day (08:00–18:00), when the ambient temperature is higher. Furthermore, as was also shown in the COP optimisation case with the standard DHW cylinder configuration, the heat pump is often operated at lower than the nominal capacity, which means that it is operated for longer periods but has a higher average system COP. Comparing Figs. 19 and 22, it is clear that the use of the SH thermal store in the advanced configuration allows for greater flexibility, since the operation of the heat pump during the night-time hours, when the ambient temperature is low, is remarkably lower.

Finally, when the objective function is self-sufficiency (Fig. 23), there is a clearer tendency to charge both the SH and DHW thermal stores preferentially during periods of high solar irradiation (09:00–15:00); with time-shifting of heat pump operation achieved more effectively than for the standard system configuration.

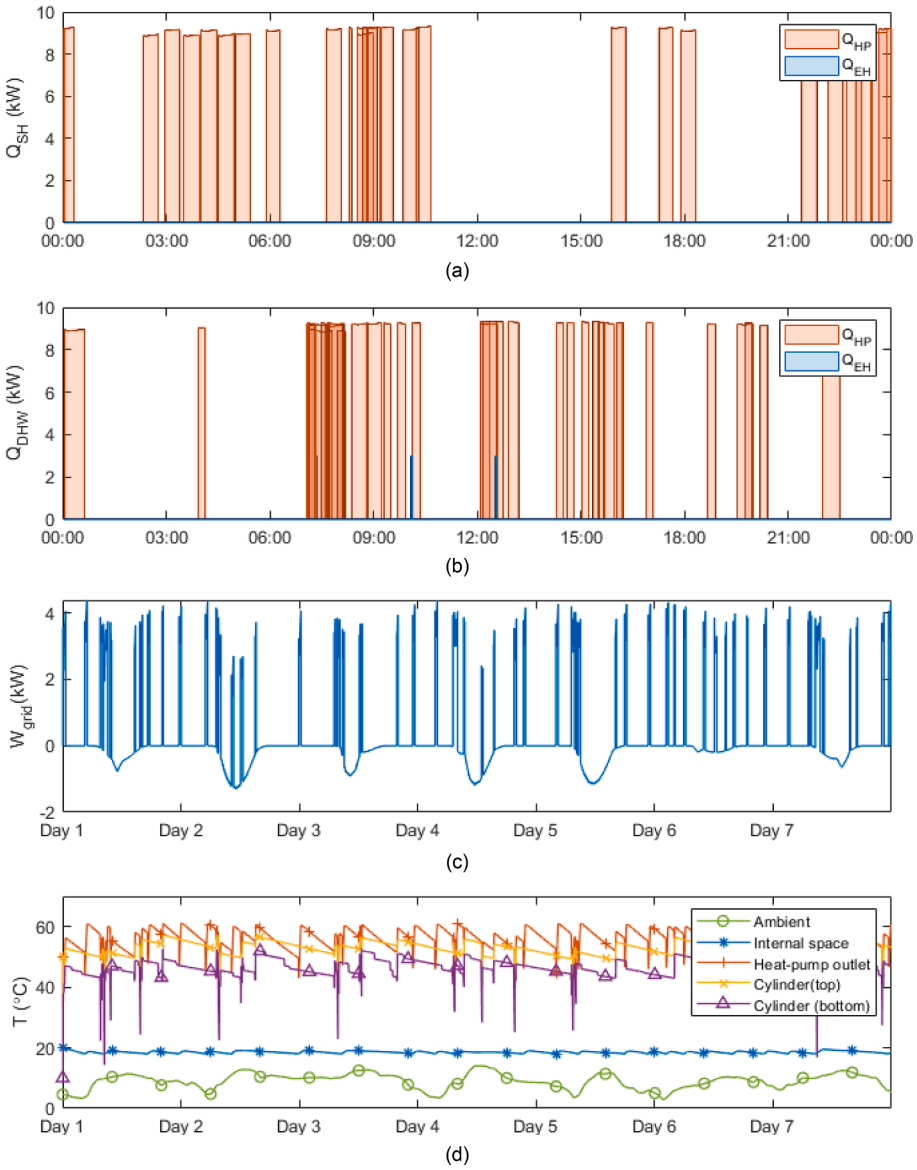

Fig. 17. Time-resolved results for the baseline case for a typical autumn in the UK location: (a) heat pump and electric heater thermal outputs for SH, where the 7 days of the week are overlayed; (b) heat pump and electric heater heat outputs for DHW, where the 7 days of the week are overlayed; (c) electricity exchanged with the grid; displayed using positive values for electricity import; (d) ambient temperature, internal space temperature, heat-pump outlet temperature, hot-water temperature at the top of the DHW cylinder and cold-water temperature at the bottom of the DHW cylinder.

3.5. Annual cost and performance analysis

The seasonal results obtained for each optimisation case and objective function are aggregated to estimate the potential improvement over a whole year and summarised in Table 3. As demonstrated, for the unoptimised baseline case with the standard heat pump and DHW cylinder configuration, the total annual cost required to meet the total heat demand for the considered household is ~ £410 in the UK location and £1060 in the German location (bearing in mind the considerably higher winter heating load for the German location). By using the same configuration but optimising the operation to minimise running cost, an annual saving of more than 20 % (£90 for the UK location and £210 for the German location) is observed. Note that the relative savings are highly influenced by the available time-of-use electricity tariffs considered for the two locations. Assuming that the lifetime of the heating system is 20 years, it is estimated that an end-user could achieve savings of up to £1800 over the system lifetime for the UK location, and up to £4200 for the German location.

The comparison of the two European locations chosen for this study shows that significant economic savings can be achieved under both mild and more extreme seasonal climate conditions. Especially for locations with high heating demand in cold winter months (such as Munich, Germany), the savings that can be achieved through flexible operation of the heat pump provide the potential to significantly improve the system's competitiveness compared to a more rigid operation that does not take advantage of the variable-rate electricity tariff.

The advanced configuration based on two PCM thermal stores, in conjunction with smart control, provides the ability to time-shift the heat pump operation for both DHW and SH. This results in even higher annual operational cost savings of £160 for the UK location and £310 for the German location, which translates to estimated savings over the system lifetime of up to £3600 and £6200 respectively.

It is worth mentioning that the rapid increase in energy prices in 2022 makes the potential cost savings from smart heat pump operation even higher. In the UK, for example, the average price of domestic electricity prices is expected to have increased by more than 40 % by the end of 2022, as compared to 2021 [70]. Based on this 40 % increase, potential savings in the UK during the heat pump lifetime could be further increased by £720 (i.e., resulting in a total of £2520) with the standard configuration and by £1440 (i.e., resulting in a total of £5040) with the advanced configuration.

In Germany, the changes in 2022 are even more severe, with energy prices increasing due to various factors. The average wholesale electricity price in August 2022 was more than five times higher than that of

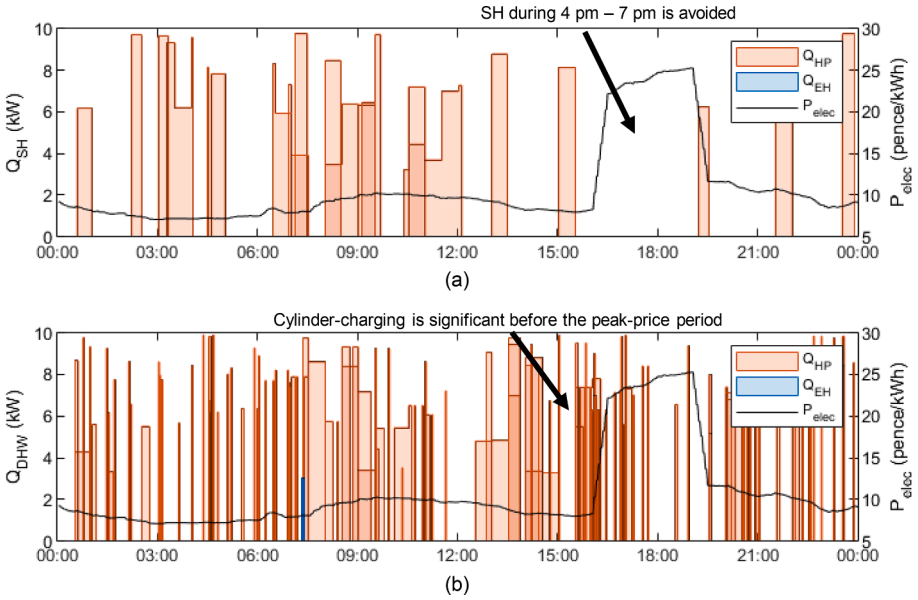

Fig. 18. Time-resolved thermal output profiles for (a) SH; (b) DHW heating, optimised for minimum operational cost with the standard heat pump and DHW cylinder configuration. Results are plotted for the typical autumn week in the UK location with thermal output profiles for all 7 days overlaid on the same plot, alongside the average daily electricity price profile for the UK dynamic time-of-use tariff.

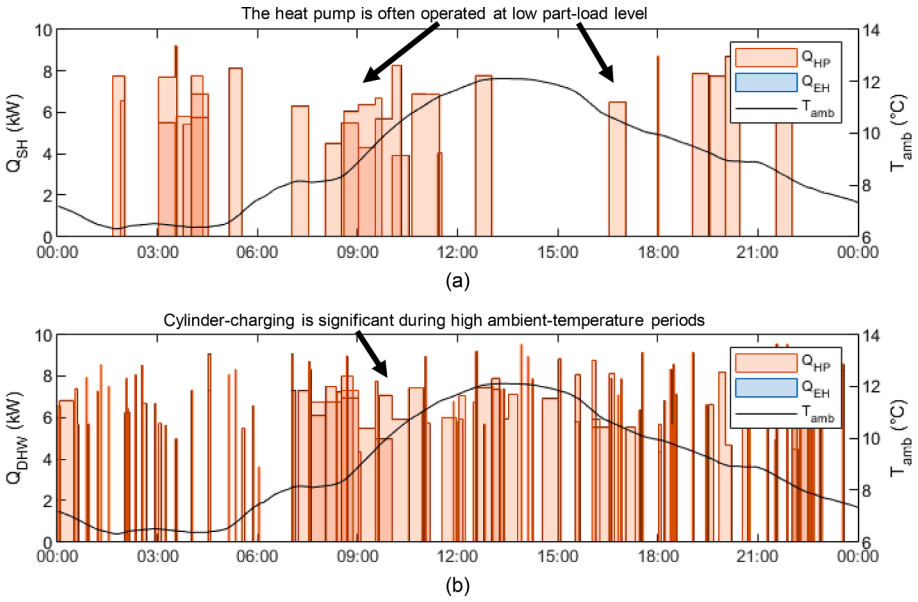

Fig. 19. Time-resolved thermal output profiles for (a) SH; (b) DHW heating, optimised for maximum COP with the standard heat pump and DHW cylinder configuration. Results are plotted for the typical autumn week in the UK location with thermal output profiles for all 7 days overlaid on the same plot, alongside the average daily outdoor-ambient temperature profile.

the previous year [71] and there is still significant uncertainty about how it will evolve in upcoming years. In our analysis, the domestic electricity prices were derived from wholesale price data. It could be expected that, without adequate government intervention, the major increase in wholesale electricity prices could soon have significant impacts on domestic consumers in Germany. In terms of heating costs, this means that smart heat pump operation strategies will become even more rewarding. A 100 % increase in domestic electricity prices in Germany, for example, could lead to potential additional savings during the heat pump lifetime of £4200 (i.e., resulting in a total of £8400) with the standard configuration and £6200 (i.e., resulting in a total of £12400) with the advanced configuration. Despite the significant uncertainty in future prices in both the UK and Europe, the findings of the operational optimisation described in this work are still relevant, and any further increases in electricity prices would lead to an even higher potential for cost savings using smart heat pump operation.

In view of maximising energy performance, the optimisation results for the standard system configuration show an estimated annual COP of 2.7 for the UK location and 2.6 for the German location, compared to baseline values of 2.5 and 2.4, respectively. For the advanced system configuration with PCM storage, the degree of COP improvement is of a similar magnitude; despite the enhanced system flexibility, the higher heat pump output temperature required to charge the SH PCM store instead of heating the space directly limits the potential for further increasing COP through optimisation. For the maximum self-sufficiency objective, the potential to time-shift the heat pump operation with both

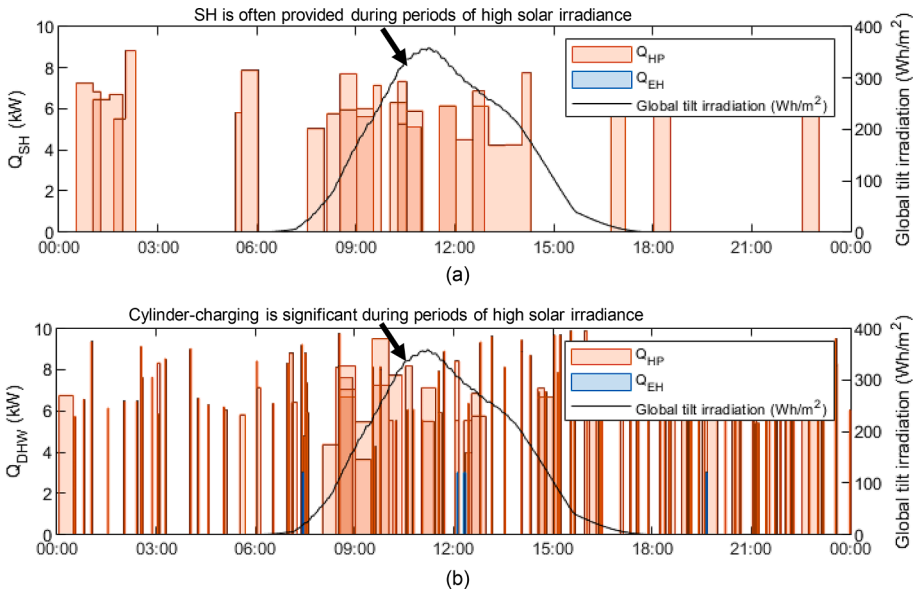

Fig. 20. Time-resolved thermal output profiles for (a) SH; (b) DHW heating, optimised for maximum self-sufficiency from PV with the standard heat pump and DHW cylinder configuration. Results are plotted for the typical autumn week in the UK location with thermal output profiles for all 7 days overlaid on the same plot, alongside the average daily solar irradiance profile at the tilted plane of the PV array.

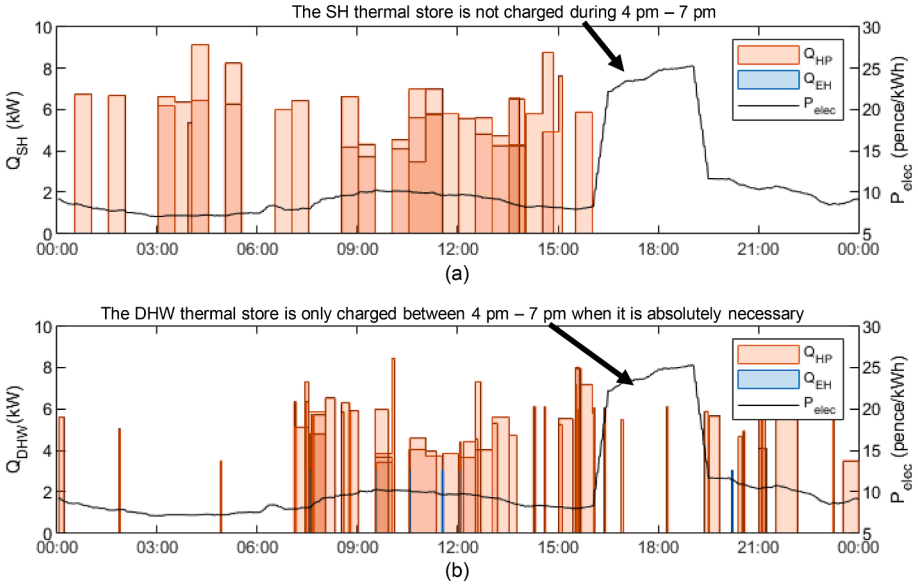

Fig. 21. Time-resolved thermal output profiles for (a) SH storage heating; (b) DHW storage heating, optimised for minimum operational cost with the advanced PCM storage configuration. Results are plotted for the typical autumn week in the UK location with thermal output profiles for all 7 days overlaid on the same plot, alongside the average daily electricity price profile for the UK dynamic time-of-use tariff.

the standard and the PCM storage configurations has a large impact on the fraction of annual demand covered by local PV, which is more than doubled compared to the baseline. Overall, these results demonstrate that, even in the absence of large thermal storage volumes (i.e., using a typical storage volume of just 200 L), average households can achieve substantial economic savings and improved energy performance.

4. Conclusions

The use of smart control strategies to operate heat pumps coupled to thermal storage has the potential to provide great value in distributed energy systems. By increasing flexibility, such strategies encourage the transition of the current electricity system to a lower-carbon grid, and provide significant economic and environmental benefits. In this paper, a detailed assessment of the potential impact of optimising the operation of domestic ASHP systems with thermal storage was performed.

The objectives considered for the optimisation were the heat pump running cost, the energy consumption (though the COP), and the fraction of the energy demand met by local renewables (self-sufficiency ratio). The operational optimisation of two different system configurations was investigated: (i) a standard configuration based on an 8.5 kW_{th} ASHP coupled to a 200-L DHW cylinder; and (ii) an advanced configuration based on an 8.5 kW_{th} ASHP coupled to two PCM thermal stores (100 L for DHW and 100 L for SH). These were compared to an unoptimised baseline case, which was taken to be the standard configuration. The work involved the development of comprehensive thermal network models for a typical house. Two locations were investigated: Oban, in Scotland, UK, which has a mild climate, and Munich, Southern

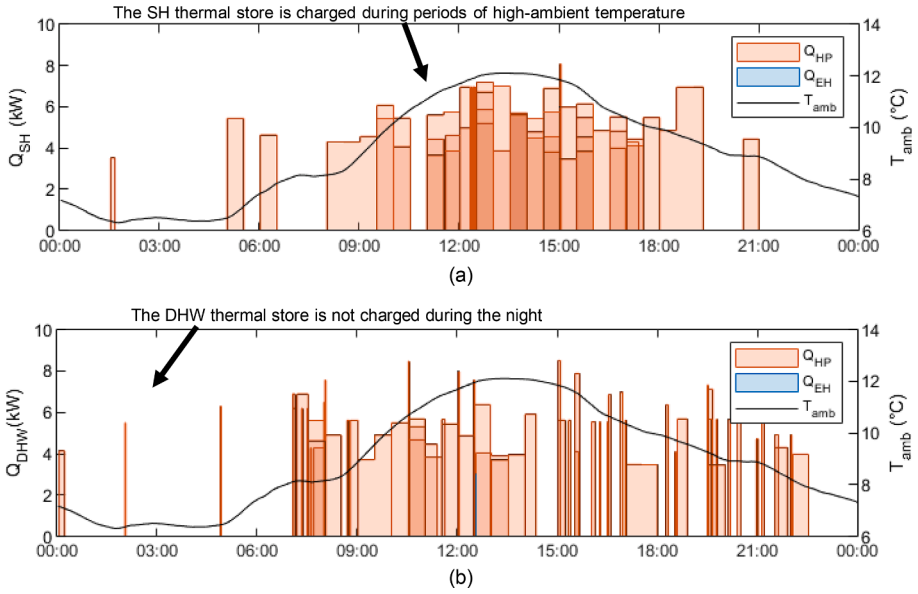

Fig. 22. Time-resolved thermal output profiles for (a) SH storage heating; (b) DHW storage heating, optimised for maximum COP with the advanced PCM storage configuration. Results are plotted for the typical autumn week in the UK location with thermal output profiles for all 7 days overlaid on the same plot, alongside the average daily outdoor-ambient temperature profile.

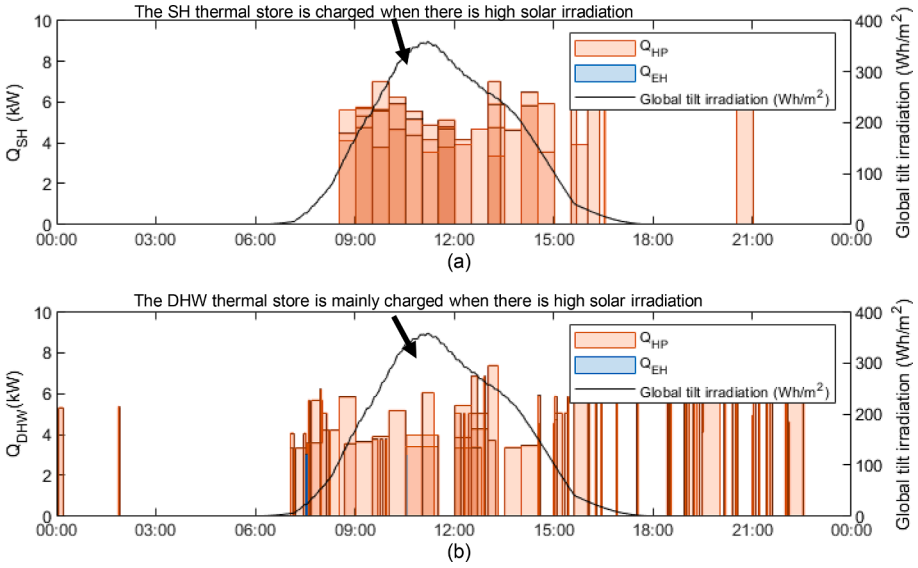

Fig. 23. Time-resolved thermal output profiles for (a) SH storage heating; (b) DHW storage heating, optimised for maximum self-sufficiency from solar-PV with the advanced PCM storage configuration. Results are plotted for the typical autumn week in the UK location with thermal output profiles for all 7 days overlaid on the same plot, alongside the average daily solar irradiance profile at the tilted plane of the PV array.

Germany, which is a sunnier location with more extreme seasonal and daily climate variations.

The results reveal that optimising the operation of a domestic heat pump with thermal storage can lead to substantial improvements in overall system performance. Depending on the chosen objectives, the operational costs can be reduced by avoiding peak electricity-price hours, the average COP of the system can be increased by operating during higher-ambient-temperature periods and often at lower capacities, and the proportion of imported electricity can be reduced by maximising the consumption of locally produced electricity, which in our study was sourced from a solar-PV system.

When the operation of the standard system configuration featuring the ASHP with a DHW cylinder was optimised for minimum operational cost, annual cost savings of over 20 % were observed at both locations compared to the baseline, amounting to £90 in the UK and £210 in Germany based on the electricity tariffs available locally. The rapid increase in energy prices in 2022 suggests that annual savings from smart operation could be significantly higher in the near future. Furthermore, the average heating demand and electricity tariff price at the German location were considerably higher than those at the UK location. When optimising for maximum COP, the seasonal average increased from 2.5 to 2.7 at the UK location, with a similar increase from 2.4 to 2.6 at the German location. When optimising for maximum self-sufficiency, the fraction of heat pump demand covered by solar-PV increased from 8 % to 16 % at the UK location, and from 6 % to 15 % at the German location. This was achieved without any electrical battery storage capacity for the PV system.

Results relating to the advanced configuration with the two PCM

Table 3
Summary of the total operational cost, average system COP and self-sufficiency for a whole year using the baseline and the two optimised cases. Results are aggregated from those of the typical autumn, winter, spring and summer weeks in UK and German locations. Each output variable reported represents the objective associated with that particular optimisation case.

Optimisation objective	Location	Baseline case: standard configuration with hot-water cylinder	Optimised case: standard configuration with DHW cylinder	Optimised case: advanced configuration with PCM DHW and SH thermal stores
Total operational cost (£)	Oban, UK	£410	£320	£250
	Munich, Germany	£1060	£850	£750
Average system COP (-)	Oban, UK	2.5	2.7	2.7
	Munich, Germany	2.4	2.6	2.5
Self-sufficiency (%)	Oban, UK	8.0 %	16 %	34 %
	Munich, Germany	6.3 %	15 %	24 %

thermal stores showed even higher potential for cost savings. By including a thermal storage volume into the SH circuit of the investigated heating systems, sufficient buffering of demand was provided, which mostly avoided heat pump operation during peak electricity-price hours. As a result, the annual cost savings were notably higher than those achieved by the optimised standard configuration with a DHW cylinder alone based on the available electricity tariffs, i.e.: 39 % (£160) in the UK, and 29 % (£310) in Germany. Furthermore, the additional operational flexibility associated with this configuration led to a significant increase in self-sufficiency, which reached 34 % at the UK location and 24 % at the German location.

This study also showed that choosing any of the three objective functions resulted in a simultaneous improvement in the other two objectives. However, using the operational cost as the objective function limited the potential for heat pump COP improvement, and using the COP as the objective function led to a significantly reduced potential for cost savings. On the other hand, the use of self-sufficiency as the objective function led to a higher fraction of demand covered by the PV system, while also achieving substantial improvements to both the running cost and COP relative to the baseline. Thus, this objective appears to provide the best trade-off in terms of overall benefits across the three performance indicators. In conclusion, this paper provides useful insights on the potential impact of optimising the control of domestic heat pump systems operating under different environmental and economic constraints. The results can be used to guide the development of smart control strategies for such applications.

CRediT authorship contribution statement

Andreas V. Olympios: Methodology, Software, Formal analysis, Investigation, Data curation, Writing – original draft, Writing – review & editing, Visualization. **Paul Sapin:** Methodology, Software, Validation, Formal analysis, Data curation, Writing – original draft, Writing – review & editing. **James Freeman:** Conceptualization, Methodology, Formal analysis, Writing – original draft, Writing – review & editing. **Christopher Olkis:** Conceptualization, Methodology, Formal analysis, Writing – original draft, Writing – review & editing. **Christos N. Markides:** Conceptualization, Methodology, Resources, Writing – review & editing, Supervision, Project administration.

Declaration of Competing Interest

The authors declare that they have no known competing financial interests or personal relationships that could have appeared to influence the work reported in this paper.

Data availability

Data will be made available on request.

Acknowledgments

The authors would like to thank Mitsubishi Electric Corporation for funding. This work was also supported by the UK Natural Environment Research Council (NERC) [grant number NE/L002515/1] and the UK Engineering and Physical Sciences Research Council (EPSRC) [grant number EP/R045518/1]. The authors would also like to acknowledge the Science and Solutions for a Changing Planet Doctoral Training Partnership (SSCP DTP). Data supporting this publication can be obtained on request from cep-lab@imperial.ac.uk. For the purpose of Open Access, the authors have applied a CC BY public copyright licence to any Author Accepted Manuscript version arising from this submission.

Appendix. PCM properties and thermal network conductance and capacitance values

The thermophysical property values used to model the PCM thermal stores are listed in Table A1. The thermal conductance and capacitance values used in the thermal network models are listed in Table A2. All values are representative of a modern, detached, 3-bedroom residential dwelling in the UK and were obtained based on information from manufacturers.

Table A1
Thermophysical property values used to model the PCM thermal stores (based on the product "PCM A48" from PCM Products ltd [51]).

Parameter	Value	Description
L_{PCM}	$230 \bullet 10^3$ J/kg	specific latent heat of PCM material
T_{PCM}	48 °C	melting temperature of PCM material
ρ_{PCM}	810 kg/m	density of PCM material

Table A2
Thermal conductance and capacitance values used in the thermal network models [54].

Parameter	Value	Description
G_{int}	95 W/K	thermal conductance between building envelope and internal environment
G_{ext}	840 W/K	thermal conductance between building envelope and external environment
G_{vent}	60 W/K	thermal conductance due to air flow between internal and external environment
G_{em}	150 W/K	thermal conductance between heat emitters and internal space
$G_{c,loss}$	2 W/K	thermal conductance of DHW cylinder insulation
$G_{p,loss}$	2 W/K	thermal conductance of pipe insulation
$\dot{V}_{PL}$	12 L/min	volumetric flowrate in primary loop
$\dot{V}_{SL}$	12 L/min	volumetric flowrate in secondary loop
ε	0.8	heat exchanger effectiveness
$\dot{Q}_{ig}$	700 W	internal heat gains due to appliances, lighting and people
C_{int}	$1 \bullet 10^7$ J/K	thermal capacitance of the internal space (air volume + furnishings)
C_{env}	$2.5 \bullet 10^7$ J/K	thermal capacitance of the building envelope
C_{em}	$2 \bullet 10^7$ J/K	thermal capacitance of heat emitters
C_{PL}	$2 \bullet 10^7$ J/K	thermal capacitance of heat pump primary flow loop

References

[1] EU Commission. Towards a smart, efficient and sustainable heating and cooling sector. Brussels, 2016. Available from: https://ec.europa.eu/commission/presscorner/detail/en/MEMO_16_311.
[2] Department of Business, Energy & Industrial Strategy. UK becomes first major economy to pass net zero emissions law. 2019. Available from: https://www.gov.uk/government/news/uk-becomes-first-major-economy-to-pass-net-zero-emissions-law.
[3] Felix B. France sets 2050 carbon-neutral target with new law. Reuters. 2019. Available from: https://www.reuters.com/article/us-france-energy-idUSKCN1TS30B.
[4] United Nations. Paris agreement. 2015. Available from: https://unfccc.int/sites/default/files/english_paris_agreement.pdf.
[5] Climate Change Committee. Next steps for UK heat policy. 2016. Available from: https://www.theccc.org.uk/publication/next-steps-for-uk-heat-policy.
[6] Secretary of State for Business, Energy & Industrial Strategy. Heat and buildings strategy. 2021. Available from: https://www.gov.uk/government/publications/heat-and-buildings-strategy.
[7] Paardekooper S, Lund RS, Mathiesen BV, Chang M, Petersen UR, Grundahl L, et al. Heat Roadmap Europe 4: Quantifying the impact of low-carbon heating and cooling roadmaps. Denmark: Aalborg University; 2018.
[8] Markides CN. The role of pumped and waste heat technologies in a high-efficiency sustainable energy future for the UK. Appl Therm Eng 2013;53:197–209.
[9] Thomaßen G, Kavvadias K, Jiménez Navarro JP. The decarbonisation of the EU heating sector through electrification: a parametric analysis. Energy Policy 2020;148:111929.
[10] ICAX. Grid carbon factors, 2020. Available from: https://www.icax.co.uk/Grid_Carbon_Factors.html.
[11] Olympios AV, Aunedi M, Mersch M, Krishnaswamy A, Stollery C, Pantaleo AM, et al. Delivering net-zero carbon heat: technoeconomic and whole-system comparisons of domestic electricity- and hydrogen-driven technologies in the UK. Energy Convers Manag 2022;262:115649.
[12] European Heat Pump Association. European heat pump market data. 2021. Available from: https://www.ehpa.org/market-data.
[13] Olympios AV, Pantaleo AM, Sapin P, Markides CN. On the value of combined heat and power (CHP) systems and heat pumps in centralised and distributed heating systems: Lessons from multi-fidelity modelling approaches. Appl Energy 2020;274:115261.
[14] Wang J, Zhong H, Ma Z, Xia Q, Kang C. Review and prospect of integrated demand response in the multi-energy system. Appl Energy 2017;202:772–82.
[15] Mazidi M, Zakariazadeh A, Jadid S, Siano P. Integrated scheduling of renewable generation and demand response programs in a microgrid. Energy Convers Manag 2014;86:1118–27.
[16] van Leeuwen RP, de Wit JB, Smit GJM. Review of urban energy transition in the Netherlands and the role of smart energy management. Energy Convers Manag 2017;150:941–98.
[17] Ma T, Wu J, Hao L. Energy flow modeling and optimal operation analysis of the micro energy grid based on energy hub. Energy Convers Manag 2017;133:292–306.
[18] Olympios AV, Le Brun N, Acha S, Shah N, Markides CN. Stochastic real-time operation control of a combined heat and power (CHP) system under uncertainty. Energy Convers Manag 2020;216:112916.
[19] Hewitt NJ. Heat pumps and energy storage - the challenges of implementation. Appl Energy 2012;89:37–44.
[20] Hoseinpoori P, Olympios AV, Markides CN, Woods J, Shah N. A whole-system approach for quantifying the value of smart electrification for decarbonising heating in buildings. Energy Convers Manage 2022;268:115952.
[21] Alva G, Lin Y, Fang G. An overview of thermal energy storage systems. Energy 2018;144:341–78.
[22] Borderon J, Virgone J, Cantin R. Modeling and simulation of a phase change material system for improving summer comfort in domestic residence. Appl Energy 2015;140:288–96.
[23] Baetens R, Jelle BP, Gustavsen A. Phase change materials for building applications: a state-of-the-art review. Energy Build 2010;42(9):1361–2138.
[24] PCM Products Ltd. PCM Solutions. 2021. Available from: https://www.pcmproducts.net/Phase_Change_Material_Products.htm.
[25] Tyagi VV, Buddhi D. PCM thermal storage in buildings: a state of art. Renew Sustain Energy Rev 2017;11(6):1146–66.
[26] Renaldi R, Kiprakis A, Friedrich D. An optimisation framework for thermal energy storage integration in a residential heat pump heating system. Appl Energy 2017;186(3):520–59.
[27] Arteconi A, Hewitt NJ, Polonara F. Domestic demand-side management (DSM): role of heat pumps and thermal energy storage (TES) systems. Appl Therm Eng 2013;51(1–2):155–65.
[28] Fischer D, Bernhardt J, Madani H, Wittwer C. Comparison of control approaches for variable speed air source heat pumps considering time variable electricity prices and PV. Appl Energy 2017;204:93–105.
[29] Le KX, Huang MJ, Wilson C, Shah NN, Hewitt NJ. Tariff-based load shifting for domestic cascade heat pump with enhanced system energy efficiency and reduced wind power curtailment. Appl Energy 2019;257:113976.
[30] Cabrol L, Rowley P. Towards low carbon homes – a simulation analysis of building-integrated air-source heat pump systems. Energy Build 2012;48:127–36.
[31] Kelly NJ, Tuohy PG, Hawkes AD. Performance assessment of tariff-based air source heat pump load shifting in a UK detached dwelling featuring phase change-enhanced buffering. Appl Therm Eng 2014;71(2):809–20.
[32] Watson SD, Lomas KJ, Buswell RA. Decarbonising domestic heating: What is the peak GB demand? Energy Policy 2019;126:533–44.
[33] Hot Water Association. Sizing a hot water cylinder. 2021. Available from: https://www.hotwater.org.uk/sizing-a-hot-water-cylinder.
[34] Samsung. Eco heating system: powerful and eco-friendly air to water solutions for heating. 2018. Available from: https://www.heatpumpsscotland.com/wp-content/uploads/2018/06/Energy-Labelling.pdf.
[35] Olympios AV, Hoseinpoori P, Mersch M, Pantaleo AM, Simpson Michael, Sapin P, et al. Optimal design of low-temperature heat-pumping technologies and implications to the whole-energy system. In: Proc: The 33rd International Conference on efficiency, cost, optimization, simulation, and environmental impact of energy systems (ECOS 2020), Osaka, Japan; 2020.
[36] Nouri G, Noorollahi Y, Yousefi H. Designing and optimization of solar assisted ground source heat pump system to supply heating, cooling and hot water demands. Geothermics 2019;82:212–31.
[37] Morrison GL, Anderson T, Behnia M. Seasonal performance rating of heat pump water heaters. Sol Energy 2004;76(1–3):147–52.
[38] Kinab E, Marchio D, Rivière P, Zoughaib A. Reversible heat pump model for seasonal performance optimization. Energy Build 2010;42(12):2269–80.
[39] Saheb Y, Shnapp S, Paci D. From nearly-zero energy buildings to net-zero energy districts: Lessons learned from existing EU projects. 2019. Available from: https://publications.jrc.ec.europa.eu/repository/handle/JRC115188.
[40] Spertino F, Fichera S, Ciocia A, Malgaroli G, Di Leo P, Ratclif A. Toward the complete self-sufficiency of an NZEBS microgrid by photovoltaic generators and heat pumps: Methods and applications. IEEE Trans Ind Appl 2019;55(6):7028–40.
[41] Irulegi O, Torres L, Serra A, Mendizabal I, Hernández R. The Ekihouse: An energy self-sufficient house based on passive design strategies. Energy Build 2014;83:57–69.
[42] Huang P, Lovati M, Zhang X, Bales C, Hallbeck S, Becker A, et al. Transforming a residential building cluster into electricity prosumers in Sweden: Optimal design of a coupled PV-heat pump-thermal storage-electric vehicle system. Appl Energy 2019;255:113864.
[43] Iwafune Y, Kanamori J, Sakakibara H. A comparison of the effects of energy management using heat pump water heaters and batteries in photovoltaic -installed houses. Energy Convers Manag 2017;148:146–60.
[44] Langer L, Volling T. An optimal home energy management system for modulating heat pumps and photovoltaic systems. Appl Energy 2020;278:115661.
[45] Herrando M, Markides CN. Hybrid PV and solar-thermal systems for domestic heat and power provision in the UK: techno-economic considerations. Appl Energy 2016;161:512–32.
[46] Vaishak S, Bhale PV. Photovoltaic/thermal-solar assisted heat pump system: Current status and future prospects. Sol Energy 2019;189:268–84.
[47] Ramos A, Chatzopoulou MA, Guarracino I, Freeman J, Markides CN. Hybrid photovoltaic-thermal solar systems for combined heating, cooling and power provision in the urban environment. Energy Convers Manag 2017;150:838–50.
[48] Mitsubishi Electric PUHZ-W85VHA2. ECODAN data book Vol 4.1, Page A-94. 2019.
[49] Samsung. EHS technical data book. 2017.
[50] DAIKIN. Altherma 3 product catalogue. 2018.
[51] PCM Products Ltd. PlusICE organic range. 2021. Available from: https://www.pcmproducts.net/files/PlusICE Range 2021-1.pdf.
[52] Underfloor Heating Systems Ltd. What is the water flow temperature? Available from: https://www.underfloorheatingsystems.co.uk/self-install-information/questions-and-answers/what-is-the-water-flow-temperature.
[53] The Mathworks. MATLAB R2021a. Massachusetts, United States; 2021.
[54] Nguyen M, Baba F, Sung A. Cold-soak testing method - based evaluation of thermal performance of a typical residential dwelling. In: Proc: The 4th International High Performance Buildings Conference, West Lafayette, USA; 2016.
[55] British Electrotechnical and Allied Manufacturers' Association. Recommended code of practice for safe water temperatures. 2020. Available from: https://www.beama.org.uk/resourceLibrary/recommended-code-of-practice-for-safe-water-temperatures—.html.
[56] Energy Saving Trust. The biggest ever review of domestic water use in Great Britain; 2013.
[57] Jordan U, Vajen K. DHWcalc: Tool for the generation of domestic hot water profiles on a statistical basis; 2017.
[58] Public Heath England. Minimum home temperature thresholds for health in winter – A systematic literature review; 2014. Available from: https://assets.publishing.service.gov.uk/government/uploads/system/uploads/attachment_data/file/776497/Min_temp_threshold_for_homes_in_winter.pdf.
[59] British Standards Institution. BS EN 14511-3:2013: Air conditioners, liquid chilling packages and heat pumps with electrically driven compressors for space heating and cooling - Test methods. 2013.
[60] Solar J. JA Solar Technology JAM6(L)-60-285/PR solar panel module product brochure; 2020.
[61] Jacobson MZ, Jadhav V. World estimates of PV optimal tilt angles and ratios of sunlight incident upon tilted and tracked PV panels relative to horizontal panels. Sol Energy 2018;169:55–66.
[62] Energy Savings Trust. Solar inverters; 2021. Available from: https://www.energysavingtrust.org.uk/sites/default/files/reports/Solar%20inverters.pdf.
[63] American Society of Heating Refrigerating and Air-Conditioning Engineers. International Weather for Energy Calculations (IWEC Weather Files). 2001. https://www.energyplus.net/weather.
[64] Octopus Energy. Introducing Octopus Agile: The 100% green electricity tariff with plunge pricing; 2020. Available from: https://octopus.energy/agile/#what-does-it-cost.

[65] aWATTar. aWATTar hourly tariff: Germany's first electricity tariff with hourly price adjustment; 2020. Available from: https://www.awattar.de/tariffs/hourly.
[66] Kalogirou SA. Solar Energy Engineering. 2nd ed. Academic Press; 2013.
[67] Reindl DT, Beckman WA, Duffie JA. Evaluation of hourly tilted surface radiation models. Sol Energy 1990;45(1):9–17.
[68] HOMER Energy. How HOMER calculates the PV cell temperature; 2021. Available from: https://www.homerenergy.com/products/pro/docs/latest/how_homer_calculates_the_pv_cell_temperature.html.
[69] British Standards Institution. BS EN 15450:2007 Heating systems in buildings – Design of heat pump heating systems; 2007.
[70] Bolton P, Stewart I. Domestic energy prices. House of Commons Library; 2022. Available from: https://commonslibrary.parliament.uk/research-briefings/cbp-9491.
[71] Statista. Average monthly electricity wholesale price in Germany from January 2019 to August 2022; 2022. Available from: https://www.statista.com/statistics/1267541/germany-monthly-wholesale-electricity-price.